The role of the central amygdala kappa opioid receptor and dopamine in discriminatory fear learning and anxiety

Madison A. Baird

A dissertation

Submitted in partial fulfillment of the

requirements for the degree of

Doctor of Philosophy

University of Washington

2020

Reading Committee:

Larry Zweifel, Chair

Charles Chavkin

Richard Palmiter

Program Authorized to Offer Degree:

Pharmacology

University of Washington

Abstract

The role of the central amygdala kappa opioid receptor and dopamine in discriminatory fear learning and anxiety

Madison A. Baird

Chair of the Supervisory Committee:

Larry Zweifel

Department of Pharmacology

Collectively, anxiety disorders are the most common mental illness in the U.S., with about 30% of Americans experiencing this disorder in their lifetime. There are a variety of anxiety disorders, including phobias, obsessive compulsive disorders, generalized anxiety, and post-traumatic stress disorder (PTSD), which display heterogeneous symptoms. Many of these disorders are based in aberrant information processing of fear-inducing stimuli. To develop new treatment options, it is necessary to identify new therapeutic targets that mediate normal and dysfunctional fear learning. While discriminative fear can be adaptive, high intensity non-discriminative generalized fear is often maladaptive and can result in fear disorders, such as post traumatic stress disorder (PTSD). Within the amygdala, the central amygdala (CeA) is highly heterogeneous, dynamic population which is critical for the acquisition, consolidation, and expression of cued fear. The CeA acts as a hub of threat discrimination information. This complex discrimination calculation is dependent on a variety of signaling molecules and neural circuits. We have previously demonstrated that CeA corticotrophin releasing hormone (CRH) expression and its local action on CRH receptor 1 (CRHR1) are necessary for the acquisition of low-threat-intensity, discriminative fear. We have also identified the critical role of VTA dopamine projections to the CeA for

maintaining cue-specific, non-generalized fear. Now, we have characterized the coexpression and localization of a variety of stress-associated neuropeptides in the CeA and identified an additional CeA signaling system that regulates anxiety and fear discrimination.

I investigated the role of kappa opioid receptor (KOR) in the CeA for regulation of conditioned threat discrimination and anxiety-like behavior in mice. We demonstrated that reduced KOR expression in the CeA, through genetic inactivation of the KOR-encoding gene (*Oprk1*) results in increased anxiety and impaired conditioned threat discrimination. KOR's endogenous ligand, dynorphin (Pdyn) is expressed locally in the CeA. Local Pdyn^{+} cells densely innervate the CeA, but reduction of CeA Pdyn through genetic inactivation of the Pdyn-encoding gene (*Pdyn*) in the CeA had no effect on anxiety or conditioned threat discrimination. However, the CeA also receives distal *Pdyn*$^{+}$ inputs from throughout the brain. When we inactivated all sources of dynorphin to the CeA we were able to recapitulate the anxiety and fear discrimination phenotypes of CeA KOR inactivation. These findings suggest that Pdyn inputs to the CeA signal through KOR to promote threat discrimination and reduce anxiety. We believe that a better understanding of this pathway and how it interacts with other stress-associated signaling molecules could aid in the discovery of new drug targets for the treatment of fear and anxiety disorders.

TABLE OF CONTENTS

LIST OF FIGURES

Part II:

Part III:

Part IV:

Part I: The study of fear and anxiety, and its biological basis

Fear and anxiety

Fear is a neurophysiological state that enables an organism to generate learned or innate defensive responses, avoid harm, and increase its chances of survival [1]. The acquisition of learned fear allows an organism to adapt to changing threats in their environment. During fear learning, a defensive response such as freezing or retreat becomes a learned response to cues that predict a noxious stimulus such as pain. Fear is often defined as an acute a defensive response to a stimulus, whereas anxiety is a broader, chronic behavioral state that does not require an acute threat to induce heightened arousal and defensive responses. While discriminative fear is adaptive, high-intensity, non-discriminative-generalized fear is often maladaptive and can result in anxiety and fear disorders [2].

Anxiety disorders are the most common mental illness in the U.S., with about 30% of Americans experiencing this disorder in their lifetime [3]. There are a variety of anxiety-related disorders, including phobias, obsessive compulsive disorders, generalized anxiety, and post-traumatic stress disorder (PTSD), which display heterogeneous symptoms. Many of these disorders are based in aberrant information processing of fear-inducing stimuli, resulting in inappropriate responses to perceived threats as well as the sustained state of apprehension known as anxiety [4].

Experimental study of fear and anxiety

The neurocircuitry underlying learned fear has been largely dissected using Pavlovian conditioning, where a previously neutral conditioned stimulus (CS) acquires a positive or negative valence through pairings with an unconditioned stimulus (US), which has an inherent valence and generates a conditioned response. After multiple pairings, the unconditioned stimulus alone elicits the unconditioned response [5]. Pavlovian, associative, fear-conditioning paradigms include cued fear conditioning, contextual fear conditioning, and fear-potentiated startle paradigms. Contextual fear conditioning is used to examine context-specific fear learning, where the contextual cues act as the CS in the absence of acute cue presentations, and is dependent on the hippocampus [6]. With fear-potentiated startle, pairing of a learned CS before a startle stimulus augments the expression of a reflexive startle response. Cued fear

conditioning is commonly used because it is simple, robust, and allows researchers to isolate and study various stages of learned stimulus-invoked fear including fear acquisition, expression, and extinction [1].

Cued fear conditioning is the process of pairing a neutral cue, such as an auditory tone, with an aversive or noxious stimulus, such as a foot shock. After repeated pairings, the organism learns that the once neutral tone is associated with the aversive event, or the US. This paradigm can be used to distinguish between discriminative and generalized fear with the use of both a shock-paired CS (CS+) a second cue tone (the CS-), which is not paired with the US. Fear outputs are measured in response to both the CS+ and the CS- to determine whether associative fear was learned and whether the fear is discriminative (specific to the CS+) or generalized (in response to both the CS+ and CS-). In rodent models, learned fear is measured as physical freezing in response to the cues.

Behavioral assays which measure anxiety-like behaviors in rodents often measure the degree of exploration versus defensive behaviors in a novel environment. A rodent is said to be exhibiting low anxiety if it displays a tendency to explore a novel environment and spend more time in spaces with higher exposure, while an animal identified as high anxiety would prefer “safer” more enclosed spaces within the arena. Stressors such as foot shock, restraint stress, or forced swim disrupt the balance between a rodent’s innate drive for exploration of novelty and their drive to seek enclosed spaces to avoid predation. Examples of these types of assays include the open-field assay, elevated-plus/zero maze, and light-dark-exploration task. Although these are very commonly used assays of anxiety, there has been growing concern that these simple assays may have poor face validity for the human experience of anxiety. Additional less common assays of anxiety can also be used to assess other aspects of anxiety such as the social interaction test and novelty-induced hypophagia, or inhibition of feeding behavior [7]. It is important to note that as anxiety refers to a protracted internal state unlike acute fear, which is detected by acute defensive responses. Therefore, any reference to anxiety in rodents is an interpretation of a greater internal state based on a collection of measured anxiety-like behaviors. Additionally, anxiety is defined as a worry or unease, including apprehensive expectation, which relies on the assumption that a rodent experiences “worry” or “anticipation”. Thus, references to “anxiety” behavior in rodents in this dissertation should be seen as shorthand for “anxiety-like behavior”.

Fear circuitry

An encounter with an acute threat increases arousal via norepinephrine and glucocorticoid release, which act centrally and peripherally on the cardiovascular system to increase heart rate, respiration, and blood pressure [8, 9]. Stress-responsive neurotransmitters such as norepinephrine and corticotrophin releasing factor (CRH, encoded by *Crh* gene) are released throughout the brain. Circuitry involved in fear is diffusely spread throughout the brain, though most regions critical for fear send and receive signals to and from the amygdala. The amygdala processes sensory input about the CS and US from regions such as sensory cortices, the thalamus, and hindbrain nociceptive regions such as the parabrachial nucleus (PBN). Fear associations are made within the amygdala, which sends outputs directly to regions involved in fear expression and physiological responses to fear; including the periaqueductal grey (PAG), hypothalamus, and brainstem [1].

The amygdala is a heterogeneous collection of nuclei located within the temporal lobe. The lateral amygdala (LA), receives auditory, visual, gustatory, olfactory, and somatosensory information about potential threats from the cortex and thalamus [2, 10]. Thalamic inputs transmit crude threat information rapidly, while cortical inputs are a slower more detailed information pathway to the amygdala [11].

The LA is thought to be a critical site for CS-US pairings and it is a major hub where inputs relaying CS and US information converge. Plasticity in the LA is necessary for the acquisition of fear associations [10] and auditory-fear conditioning enhances the magnitude of evoked firing in LA neurons in response to fear-associated stimuli. During auditory-fear conditioning, inputs from the auditory and multimodal thalamus and the ventral auditory cortex to the LA are critical for transmitting information about complex auditory stimuli [1]. The transmission of US pain and threat information to the LA is less clear, but appears to be dependent on inputs from the spino-thalamic tract, and indirectly from the periaqueductal gray (PAG) [12]. The LA preferentially responds to unexpected or startling stimuli, and an unexpected and intense US provides a large prediction error and strong teaching signal, which results in plasticity [1].

The LA relays information to the basal amygdala (BA), which combined with the LA forms the basolateral amygdala (BLA). Threat-information processing is continued in the BA, which has reciprocal connections

with the ventral hippocampus and prelimbic cortex, and where connections with the striatum orchestrate instrumental behaviors such as escape [1, 2]. Largely inhibitory intercalated cells (ITCs) receive input from the BLA and the LA, BA, and ITCs then project to the central amygdala (CeA). The LA and BA, respectively, send projections to the lateral (CeL) and medial subdivisions (CeM) of the CeA [10]. The capsular subdivision (CeC) receives inputs from the BLA, CeL, and extra-amygdalar sources such as the PBN, which provides a critical input conveying nociceptive US information [13, 14].

In addition to amygdalar inputs, the CeA, like the LA, receives cue information directly from the auditory thalamus and cortex including auditory cortex and sensory cortices, the insular cortex, and infralimbic cortex [15]. The paraventricular thalamus (PVT) [16], bed nucleus of the stria terminalis (BNST) [17], and the parabrachial nucleus (PBN) [14, 18, 19] provide additional emotional information. The CeA further processes threat information and transforms these signals into defensive behavioral and physiological responses [20], which are generated via projections out of the amygdala. Defensive responses are mediated by projections from the CeA to the bed nucleus of the stria terminalis (BNST), parabrachial nucleus (PBN) [21], periaqueductal gray, paraventricular thalamus (PVT) [22], the hypothalamus, and the brainstem [2, 15]. Additionally the CeA mediates emotional responses to stress and fear with projections to epinephrine, serotonin, dopamine, and acetylcholine neuromodulatory systems [2].

Central amygdala fear circuitry

The CeA is the major output region of the amygdala, critical for the generation of defensive behavioral and physiological responses [20]. Research over the last decade has revealed that it is a highly heterogeneous and dynamic population that is critical for the acquisition, consolidation, and expression of cued fear [23-25] and anxiety [26, 27]. The CeA is a critical site for associative fear learning, and undergoes plasticity after fear conditioning which is necessary for learning [22-24, 28]. This largely GABAergic region has dense and varied expression of peptides and receptors known to respond to or modulate stress, such as CRH, dynorphin, enkephalin, and neurotensin [13, 29].

Within the CeA, the CeL is a heterogeneous population necessary for fear acquisition [23]. The CeL contains a high degree of locally arborizing neurons that create networks of reciprocal inhibition between

populations [23, 25]. Two major distinct CeL populations have been identified, based on their responsivity to threat-predictive cues and genetic expression. In 2010, *in vivo* electrophysiology experiments determined that there were two major groups of cells identified in CeA recordings, cells that became active in response to a learned CS (CeL_{on}) and cells that became inhibited (CeL_{off}) [23]. It was identified that these CeL_{off} cells largely correspond to protein kinase C-δ expressing cells (PKCδ+, *Prkcd gene*), which reciprocally inhibit and are inhibited by *PKCδ*- cells [25]. It was later determined that a major population of PKCδ- cells which increase their firing rate during CS exposure (CeL_{on}) express somatostatin (*Sst*+) [30]. Both CeL_{on} and CeL_{off} neurons send projections outside of the amygdala as well as unidirectional projections to the CeM [23], though CeL_{off} neurons apply functional tonic inhibitory control to CeM fear output [25]. The CeM is responsible for fear expression. Electrical stimulation of the CeM induces immediate and non-conditioned freezing [23] as these neurons send direct projections to various fear output structures, detailed above.

The third subregion of the CeA is the capsular CeA (CeC). Fear circuitry in the CeC is less characterized, but this subregion is well recognized for its role in pain. The CeC is known to receive critical inputs conveying nociceptive information from the spinal cord, and brainstem through the parabrachial nucleus (PBN) [14, 31] and the majority of its cells are responsive to noxious stimuli [32]. *PKCδ*+ cells are also present in the CeC and likely make up a portion of the freezing-off CeL_{off} population, as researchers often do not distinguish between the CeC and CeL *PKCδ*+ populations. These two spatially close *PKCδ*+ populations might have distinct roles in fear, as one group demonstrated that optogenetic stimulation of CeC *PKCδ*+ cells induces unconditioned freezing, while CeL *PKCδ*+ stimulation does not [13].

The CeA orchestrates fear discrimination

Discriminative fear can be defined as learned fear of specific cues which have previously predicted a threat. Fear generalization, on the other hand, often involves intense and excessive fear, where learned fear is not specific to a particular threat-predicting cue. This inappropriate and non-specific fear state is

associated with heightened arousal and anxiety [27] and can result in fear and anxiety disorders such post-traumatic stress disorder or generalized anxiety.

The CeA acts as a hub of threat discrimination information, directly receiving cue information from extra-amygdalar regions such as sensory cortices and the thalamus, as well as neuromodulatory inputs such as ventral tegmental area (VTA) dopamine projections [33]. Dopamine receptor activation in the CeA is necessary for fear learning [34, 35], and time-locked inhibition of CeA dopamine release or partial block of dopamine signaling results in dysregulated fear responses. Dopamine inputs to the CeA signal the level of certainty that a cue is threat-predictive [36]. CeA dopamine D2 receptor (D2R) blockade, or inhibition of VTA dopamine inputs to the CeA during cue presentation, results in fear generalization [36, 37]. This suggests that the CeA circuits are critical for the tuning of both fear intensity and specificity.

As discussed above, plasticity occurs in the CeA following fear conditioning, inducing changes in both tonic and phasic firing of neurons. Animals exhibiting cue generalization demonstrate differential plasticity in CeM, CeL_{on}, and CeL_{off} neurons compared to discriminating animals [23]. Decreases in extra-synaptic inhibition onto CeL_{off} neurons correlate with intensity of fear generalization [27]. Thus, a better understanding of distinct populations within the CeA, their responses to fear conditioning, and their role in discriminative and generalized fear may facilitate our understanding the transition from adaptive to maladaptive fear acquisition.

Part II: Characterization of CeA stress-associated neuropeptide populations

Stress-associated CeA neuropeptides

The CeA contains numerous subpopulations that express various fear and anxiety-related peptides including corticotrophin releasing factor (encoded by the *CRH* gene), dynorphin (*Pdyn*), neurokinin B (*Tac2*), neurotensin (*Nts*), and neuropeptide Y (*Npy*) [29]. All of these CeA peptides have been shown to play some role in acquisition, consolidation, or expression of fear, anxiety, or other stress-regulated behaviors such as ethanol consumption [38-42].

CeA CRH is a stress-responsive molecule, as threat and subsequent glucocorticoid release results in increases in CeA *CRH* mRNA [43]. We have recently shown that CeA CRH expression and CRH receptor 1 (CRHR1, *Crhr1* gene) activation are necessary for the acquisition of discriminative fear learning at low threat intensities, but unnecessary for the acquisition of high-intensity-generalized fear. CeA CRH^+ cells have a notable expression pattern. In the anterior CeL, *CRH*-expressing neurons were identified to form a dense cluster of neurons somewhat distinct from previously identified *Sst* and *Prkcd* expression [39]. CeA CRH neurons primarily send local projections throughout the CeA, where there are a large number of Crh-receptor 1 (*Crhr1*) expressing cells and comparatively low levels non-local CRH inputs. This spatial characterization of CRH and CRHR1 expression patterns in the CeA has been extremely useful for modeling and understanding CRH's role in CeA fear circuits.

The kappa opioid receptor (KOR, encoded by *Oprk1*) is an additional stress-associated protein expressed in the CeA [44]. KOR is a $G_{\alpha i}$-coupled G-protein coupled receptor that induces analgesia, dysphoria, and anxiety upon global activation by intracerebroventricular (ICV) or intraperitoneal (IP) injected agonist [45], such as synthetic U50 or its endogenous ligand dynorphin. The prodynorphin (*Pdyn*) gene expresses a precursor protein that undergoes cleavage into multiple active peptide products including dynorphin A, dynorphin B, α-neo-endorphin, and β-neo-endorphin [46]. Dynorphin activation of KORs is believed to encode the dysphoric component of stress, and global activation of its receptor, KOR, increases depression-like behaviors, anxiety, and pro-addictive behaviors [47]. Dynorphin also mediates a variety of

adaptive responses to stress, such as analgesia and aversion, which respectively increase physical ability and motivation to escape from a threat [48].

KOR signaling modulates CRH synaptic effects throughout the brain, and appears to mediate some of CRH-induced behaviors. It has been previously demonstrated that ICV CRH-induced anxiety and aversion is blocked by IP injection of KOR antagonist, norBNI, or by *Pdyn*-gene knockout [45, 49]. Thus, ICV CRH induced anxiety appears to depend on dynorphin, and its activation of KOR.

We decided that in order to develop a good understanding of KOR's role in CeA-mediated fear and anxiety behaviors, we needed to further characterize KOR^+ and $dynorphin^+$ cell locations, gene expression, and circuitry. This characterization would be more complete with an understanding of how Pdyn-KOR may interact with other stress-related neuropeptide systems.

Characterization of CeA neuropeptide expression

To study the behavioral role of CeA neuropeptide populations, such as Pdyn-KOR, we wanted to establish a better understanding of CeA peptide and neuromodulator populations. When we started this project, little was known about the particular cell populations in the CeA other than *Sst*+ and *Prkcd*+ cells. It was known that the CeA expressed a wealth of neuropeptides and receptors, and we decided that it would be important to characterize the spatial location and gene expression profile of *Pdyn*+ and *Oprk1*+ cells as well as stress-associated neuropeptide populations.

First, we used the RiboTag technique to investigate overlapping populations within the CeA. RiboTag is a cell-specific RNA isolation technique which allows us to precipitate ribosomes with actively translating mRNAs, specifically from Cre-expressing cell populations. RiboTag works by expressing a ribosomal protein tagged with hemagglutinin A, RPL22-HA, that allows for cell-type-specific immunoprecipitation of ribosomes [50]. We injected an adeno-associated virus (AAV) containing double-floxed inverted open reading frame (FLEX)- RPL22-HA into the CeA of *Pdyn*-Cre, *Tac2*-Cre and *Nts*-Cre animals; which allowed us to isolate RNA from specific CeA populations based on their gene expression.

Pdyn-, Tac2- and *Nts*-expressing populations displayed enrichment of all three of these transcripts plus *Crh*, suggesting a degree of coexpression (Figure 1A-C). While these populations did not show a high degree of enrichment for *Sst,* compared to surrounding cells*, Sst* transcript was expressed more highly than any other mRNA probed. Thus, Sst is likely expressed in these populations but is not specific to *Pdyn*+ *Tac2*+ or *Nts*+ populations in and nearby the CeA. *Pdyn*$^{+}$ cells showed expression of *Crhr1* and *Oprk1*, but expression was not enriched compared to the rest of the CeA. Transcripts were considered enriched in a population if their average fold-enrichment score was 2 or more, and de-enriched if their average fold-enrichment score was less than 1. Thus, we noted that *Oprk1* was enriched in *Pdyn*+ populations, but was de-enriched in *Nts*+ and *Tac2*+ populations. This finding supports that these peptide-expressing populations are partially overlapping, but do not form one homogenous population.

Figure 1

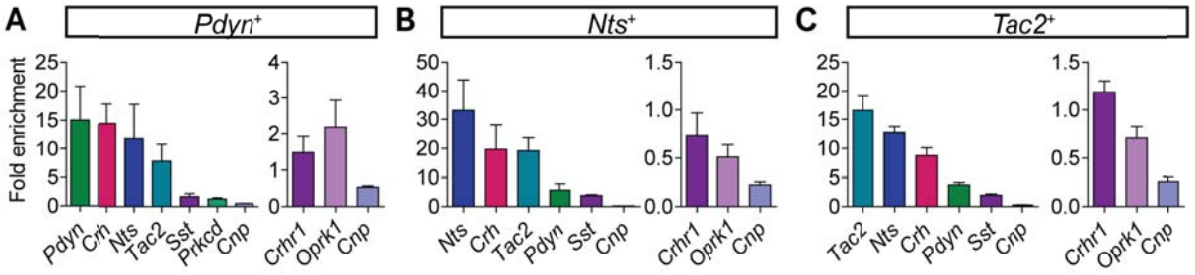

Figure 1: Neuropeptides Pdyn, Nts, Tac2, and Crh are coexpressed in the CeA
(A-C) RiboTag analysis of mRNA isolated from A) *Pdyn*, B) *Nts*, and C) *Tac2*-expressing CeA populations reveils co-expression. Fold enrichment is a comparison of normalized mRNA in the target population (ip) versus the entire CeA sample(input). A fold enrichment of 1 suggests that the avg amount of a gene transcript per cell is the same between the ip and input). *Cnp* (2',3'Cyclic-nucleotide 3'phosphodiesterase) is a non-neuronal de-enrichment marker. Receptors, *Crhr1* and *Oprk1,* are graphed separately from peptides.

To visualize mRNA expression in the CeA, we used *in situ* hybridization (RNAscope). It was determined that *Oprk1* transcript is expressed throughout the CeA, in all three subregions (the CeC, CeL, and CeM). On the anterior to posterior axis, *Oprk1* expression is highest in the mid-CeA around -1.43 mm from bregma (Figure 2A-B). *Oprk1* expression is densest in the CeL, but the CeM has the most *Oprk1*+ cells dispersed throughout the large subregion (Figure 2C-E). We also performed *in situ* hybridization for *Pdyn* transcript and found it expressed throughout the CeA, spanning the entire anterior to posterior axis

(Figure 3A). *Pdyn* shows the highest total expression in the CeL, though *Pdyn* expression in all three subregions significantly changes along the anterior to posterior axis (One-way ANOVA CeC ***p<0.001, CeL *p=0.05, CeM ***p<0.0001). CeC and CeL expression increases and CeM expression decreases as you move posterior through the CeA (Figure 3B). In addition to *in situ* hybridization, we also visualized *Pdyn*-Cre expression with fluorescent histology. We injected AAV1-FLEX-mCherry into the CeA of *Pdyn*-Cre animals and found that expression of mCherry had a similar pattern of expression and number of cells per section. This histology experiment also confirmed the *in situ* hybridization finding that *Pdyn* expression is the highest in the CeL around -1.61 to -1.67 mm from bregma (Figure 3D-E).

We did not quantify fluorescent histology for *Oprk1*-expressing cells because the *Oprk1*-Cre mouse line injected with AAV1-FLEX-mCherry or AAV1-FLEX-KASH-GFP labeled vastly more CeA cells than *in situ* hybridization, suggesting that our *Oprk1*-Cre mouse line may have had aberrant Cre expression. Other labs have used this animal line to visualize *Oprk1* in other brain regions without issue [51], but we chose not to present any data obtained with this mouse line until we could prove that Cre was exclusively expressed in *Oprk1* expressing cells in the CeA.

Figure 2

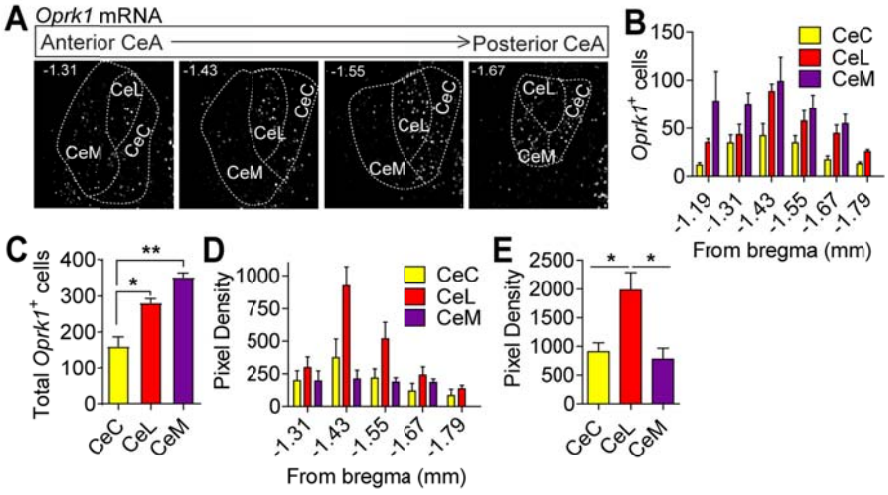

Figure 2: KOR (*Oprk1*) is expressed throughout CeA subregions
(A) Example images of RNAscope *in situ* hybridization targeting *Oprk1* gene from the anterior to posterior central amygdala.
(B) The number of *Oprk1*+ cells was quantified across 6 sections from -1.19mm to -1.79mm from Bregma, corresponding to page 41-46 of the Paxinos and Franklin mouse atlas.
(C) Significantly more cells in the CeM and CeL subdivisions express *Oprk1* compared to the CeC (One-way ANOVA $F(2,3)=30.23$ *P<0.05; Tukey's multiple comparisons test, *P<0.05, **P<0.01).
(D) Pixel density of *Oprk1* expression was calculated as [(sum of the values of the pixels)/area].
(E)The CeL had the most dense expression of *Oprk1* transcript
(One-way ANOVA $F(2,9)=8.56$ **P<0.01; Tukey's multiple comparisons test, *P<0.05)

Figure 3

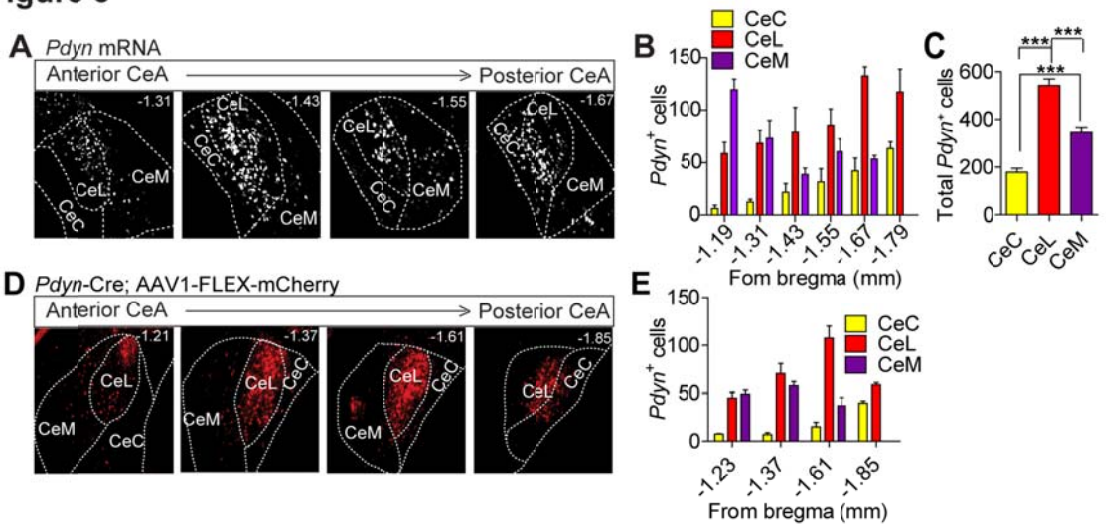

Figure 3: CeA dynorphin (*Pdyn*) is largely expressed in the CeL
(A) Example images of RNAscope *in situ* hybridization targeting *Pdyn* gene from the anterior to posterior central amygdala.
(B) The number of *Pdyn*$^+$ cells was quantified across 6 sections from -1.19mm to -1.79mm from Bregma, corresponding to page 41-46 of the Paxinos and Franklin mouse atlas (n=5).
(C) The most *Pdyn*$^+$ cells are in the CeL, followed by the CeM, then the CeC. (n=5) (One-way ANOVA $F(2,12)=67.34$ ***P<0.001; Tukey's multiple comparisons test, *P<0.05, ***P<0.001).
(D-E) The *Pdyn* Cre mouse line was verified to have a similar pattern of expression and *Pdyn* Cre$^+$ cell number compared to *Pdyn* transcript (n=3). 4 sections were quantified corresponding to -1.21, -1.37, -1.61, and -1.85 mm from bregma.

Discussion: *Oprk1* is enriched in CeA *Pdyn*$^+$ cells, but they have divergent patterns of expression

Our enrichment data suggested that Pdyn, Tac2, Nts, and Crh populations are highly overlapping in the CeA. This finding was largely supported by work published in 2017 and later [13, 52] where the authors used *in situ* hybridizations to quantify percent overlap between populations. They showed that Pdyn, Crh, Sst, Nts, and Tac2 populations have a high degree of overlap (>50% overlap between any two genes), especially in the CeL. In 2020 another group used *in situ* hybridization to compare Pdyn and Oprk1 expression [53]. The authors stated that they found little overlap between these populations, though their data reveal that about 40% of CeL *Oprk1*$^+$ cells coexpress with *Pdyn*. Additionally, various groups have demonstrated that the large majority of CeA *Sst*$^+$ cells express *Pdyn* [13, 54]. It is likely that we were unable to visualize this high degree of coexpression due to CeA-targeting punches capturing cells from regions which surround the CeA. The adjacent caudate putamen has high levels of *Pdyn*, but little *Sst*; while the basolateral amygdala and the medial amygdala widely express *Sst* with little *Pdyn [29]*.

The partial overlap between *Pdyn* and *Oprk* cells, suggested by our RiboTag data and further quantified with *in situ* hybridization by other groups [53], suggests that KOR could regulate the activity of *Pdyn*$^{+}$/*Sst*$^{+}$ CeL_{on} cells whose activation is known to be necessary for fear freezing behavior.

My RiboTag findings emphasize the necessity for targeted gene mutation studies over cell silencing to better understand the role of neuropeptide signaling in the CeA. For example, silencing the CeA *Pdyn*$^{+}$ population using tetanus light chain toxin, DREADDs, or optogenetics would block dynorphin release as well as a significant portion of NkB (*Tac2*), Nts, and CRH release, not to mention GABA. Thus, experimental silencing of these populations can inform researchers which cells are necessary or sufficient for a phenotype, but it gives little suggestion to the molecules critically involved in these diverse populations.

Additionally, we identified the spatial and subregion localization of *Pdyn* and *Oprk1* expression in the CeA. Using *in situ* hybridization and histology experiments we further characterized *Pdyn* and *Oprk1* expression patterns to reveal that both genes are expressed throughout the anterior, mid, and posterior CeA. *Pdyn* cells are highly and densely expressed in the CeL, with some dispersed expression in the CeM. This pattern of expression is nearly identical to reported patterns of *Sst* expression, which is known to highly overlap with *Pdyn* in the CeA [54, 55]. *Oprk1* expression is more dispersed throughout CeA. Oprk1 has dense expression of transcript in the CeL, but the larger CeM contains more total *Oprk1* expressing cells. KOR activation is known to reduce synaptic transmission and hyperpolarize a portion of CeM cells [56-58]. Its verified expression throughout the CeM suggests that KOR may play a critical role in reducing excitation of CeM projection neurons, and thus controlling fear output from the amygdala. Therefore, we hypothesized that specific knockout of CeA *Oprk1* could result in a heightened or dysregulated fear response.

Part III: The role of CeA dynorphin and KOR in fear and anxiety behavior

Known role of KOR signaling in fear

The role of CeA KOR in fear learning is currently poorly understood. A study demonstrated that global KOR agonism facilitates context-dependent fear renewal [59], suggesting a possible role for KOR in fear in addition to its well-studied role in anxiety. Additionally, another group demonstrated that CeA infusion of long-lasting KOR antagonist 24 hours before fear-potentiated startle lead to temporary decrease in startle response within some time blocks [40]. In the CeA, dynorphin is known to increase its expression after acute stress [55, 60, 61] or local application of CRH [62]. Some progress has been made in assessing the role of CeA dynorphin-KOR circuitry in fear-potentiated startle [40] and cued fear learning [41], but very little is known about its potential role in threat discrimination and generalization.

CeA KOR modulates CRH signaling, which is critical for fear

CeA CRH is necessary for acquisition of discriminative fear [39]. In the CeA, CRH action may elicit KOR activation through the induction of dynorphin release. CRH microinjection into the CEA has been shown to locally increase dynorphin A (1-8) [62]; however, CeA CRH modulation of other dynorphin cleavage products, many which are more specific to and efficacious at KOR, has not yet been investigated. CeA KOR appears to modulate CRH-induced synaptic effects downstream of CRH action. An electrophysiology study demonstrated that bath application of CRH activates CRHR1, eliciting increases in frequency of mini-post synaptic currents (mIPSCs) in the CeA. This CRH-induced presynaptic amplification of local GABA release was enhanced in KOR-knockout tissue or upon norBNI infusion [58], suggesting that CeA KOR action is downstream and opposing of CRH action. CRHR1 enhances synaptic transmission, likely through a stimulatory $G_{\alpha s}$- or $G_{\alpha q}$-coupled mechanism [39, 43], which appears to be subsequently attenuated with presynaptic inhibition by $G_{\alpha i}$-coupled CeA KOR.

Much is still unknown about how KOR signaling influences CeA circuitry and modulates stress signals. Though, CeA KOR modulation CeA CRH, a known regulator of discriminative fear, strengthens the hypothesis that CeA KOR might play a role in fear learning. This report that CRHR1 and KOR may have opposing synaptic effects within the CeA is intriguing, and counterintuitive given that we know KOR is

necessary for some CRH effects in other brain regions. Based on these reports and the location of KOR expression, we hypothesized that knockout of CeA *Oprk1* might have very different effects on discriminative fear than CRH, possibly resulting in enhanced or dysregulated fear expression.

CeA KOR is necessary for discriminative fear and normal baseline anxiety

To investigate the role of CeA KOR in anxiety and fear learning, we utilized *Oprk1* floxed mice to reduce KOR expression in the CeA by genetic inactivation of the KOR encoding gene *Oprk1* (*Oprk1* or KOR KO). We hypothesized that KOR KO animals would show enhanced fear and anxiety responses due to a reduction in KOR-mediated inhibition of CeM-output cells.

AAV1-Cre-GFP was injected bilaterally into the CeA of *Oprk1*$^{lox/lox}$ animals (Figure 4A), resulting in a significant reduction of *Oprk1*+ cells in the CeA (Figure 4B-C). All animals used for behavior underwent histology checks to confirm that the virus displayed a bilateral CeA hit without targeting surrounding regions such as the basolateral amygdala or the caudate putamen. Extra-CeA targeting or low levels of viral expression in the CeA usually resulted in 30-50% of the data being removed from experiments. Anxiety-like behavior was measured on the elevated plus maze (Figure 4D), where CeA KOR KO animals increased their time spent in the closed arms and reduced time spent in the open arms compared to controls, reflecting an increase in anxiety-like behavior (Figure 4E-F). This increase in anxiety was significant at baseline before the animals experienced stress during fear conditioning, but not after (Figure 4G). Both KOR KO animals and controls displayed high-anxiety behavior after shock training, but KOR KO animals showed a trend toward a longer latency to enter the open arm ($p=0.056$) (data not shown).

The next day the animals started low-threat-intensity, discriminative fear conditioning (Figure 4H). During training, the animals were exposed to two days of 10 pairings of a CS+ auditory tone and 0.3-mA foot shock, and 10 CS- tone presentations that were never paired with shock. Baseline and probe trials were tested in a separate context where the animal was exposed to 3 presentations of both the CS+ and CS- tones. Given that KOR KO resulted in baseline anxiety, and KOR's localization, we hypothesized that CeA KOR KO animals would either show increased freezing to the CS+ shock-paired cue or cue generalization including increases in freezing to the CS- tone. Animals underwent shock training and

KOR KOs had a normal velocity in response to foot shock (Figure 4I). Both groups displayed learning during shock training with increased freezing to the cues (Figure 4J-K). KOR KOs trended toward heightened CS+ freezing during shock training compared to controls, with the strongest trend on day 2 (Figure 4L).When probed in a separate non-shock context, KOR KO animals expressed normal learned CS+ freezing, but demonstrated elevated freezing to the CS- so that, unlike controls, they were no longer significantly discriminating between the shock paired and no-shock tones (Figure 4M-N).

This combination of increased baseline anxiety and generalization of learned fear was particularly compelling as many human mental health disorders such as obsessive-compulsive disorder, panic disorder, generalized anxiety disorder, and PTSD display both generalized anxiety and fear generalization [63].

Figure 4

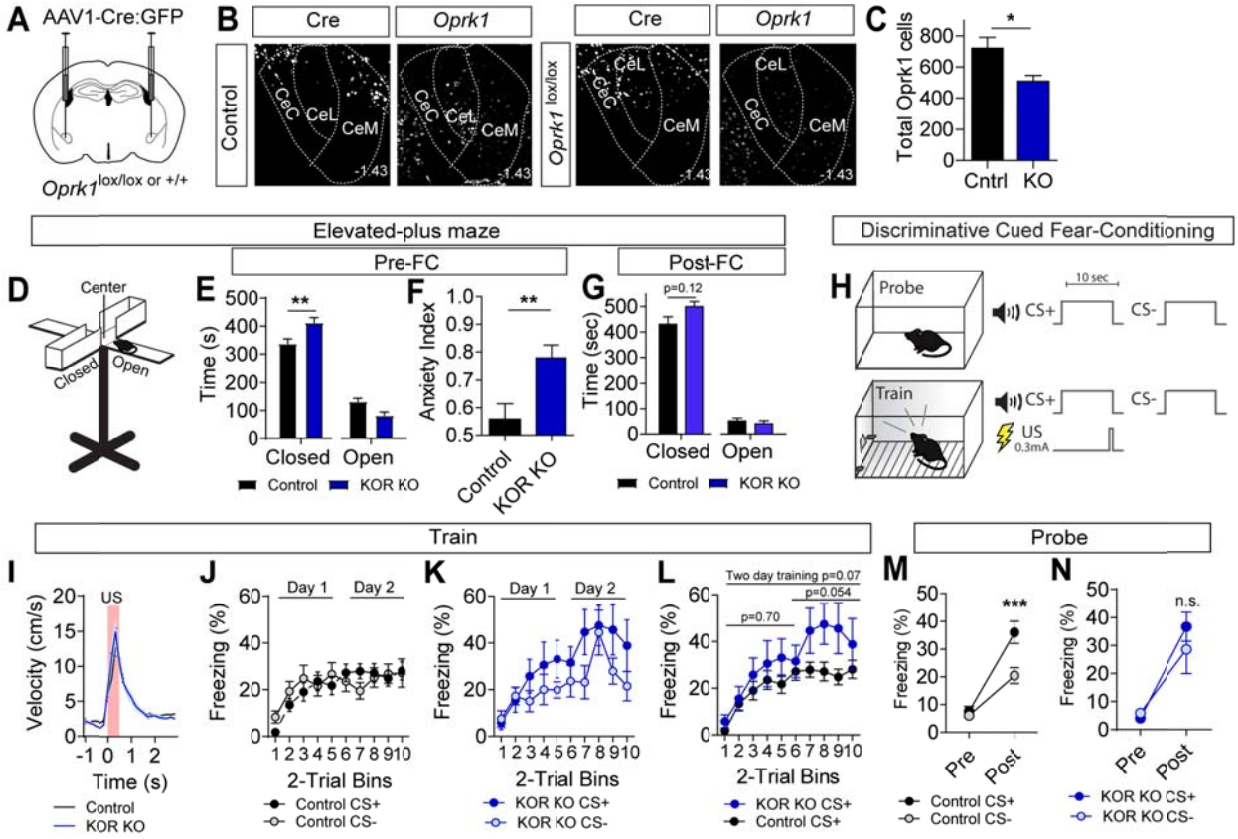

Figure 4: CeA KOR (Oprk1) knockout results in increased anxiety and fear generalization

(A) Schematic of AAV1-Cre:GFP bilateral injection into the CeA of *Oprk1*$^{lox/lox}$ mice (KOR KO) or wild type (control) mice.

(B-C) Example *in situ* hybridization shows Cre and *Oprk1* expression in the CeA and a significant reduction in *Oprk1*+ cells (n = 4-5 injections) (unpaired t-test *P<0.05), resulting in about a 30% knockout of CeA *Oprk1*. Quantification is from 4 sections from -1.31 to -1.67 mm from bregma.

(D) Schematic of the elevated-plus maze, where increased time spent in closed arms of the maze reflects increased anxiety behavior.

(E-G) CeA KOR KO animals spent increased time in the closed arms of the maze (n=10-21) (unpaired t-test *P<0.05) and showed an increase in their anxiety index, which is calculated as 1- ((open arm time)/(closed arm time)) (unpaired t-test **P<0.01). 3 days post-fear conditioning, animals show increased time in the closed arm compared to pre-condiitoning (unpaired t-test **p<0.01), but are no longer significantly different between groups.

(H) Discriminative cued fear-conditioning paradigm. In the probe context, 10-sec CS+ and CS- tones are presented with no shock. In the training context, the CS+ tone co-terminates with a 0.5-sec, 0.3-mA foot shock. After 10 CS+-shock pairings on day 1 and 2, the post training probe occurs on the third day.

(I) Velocity in reponse to foot shock was not altered by KOR KO during the 0.5-sec footshock or the two seconds after shock onset (Two-way ANOVA p>0.05) (n=10-21 for all training and probe).

(J-L) Control and KOR KO animals increased freezing to the cues throughout two days of shock training (Two-way ANOVA, effect of time, ***P<0.001). Acquisition of CS+ freezing was not significantly different between groups over the two days (Two-way ANOVA p=0.07), but on day 2 KOR KO animals display a strong trend toward heightened CS+ freezing (Two-way ANOVA p<0.054).

(M-N) : Control and KOR KO both show increased freezing to the cues after shock training (Two-way ANOVA, effect of time ***p<0.001), but KOR KO animals do not discriminate between CS+ and CS- cues (Two-way ANOVA, bonferroni post test ***p<0.001, n.s. p>0.05).

Investigation of the source of CeA dynorphin mediating normal fear and anxiety

These findings suggest that CeA KOR signaling is necessary for preserving normal baseline levels of anxiety and discriminative fear, but the source of dynorphin ligand was unknown. The CeA is known to have dense local CeL dynorphin expression (Figure 3), and due to the high level of local connectivity in the CeL and to the CeM [10] we hypothesized that this was an ideal population to investigate.

To determine the projections of CeA *Pdyn*$^{+}$ cells, we injected AAV1-FLEX-Synaptophysin-EGFP into the CeA of *Pdyn*-Cre animals. This virus labels cell bodies and terminals, allowing us to visualize where CeA *Pdyn*$^{+}$ cells synapse both locally in the CeA and outside of the amygdala. We identified the bright and dense projections locally in the CeL and CeM; in addition to distal projections to the bed nucleus to the stria terminalis (BNST), substantia nigra (SN), the midbrain reticular nucleus (MRN), and the parabrachial nucleus (PBN) (Figure 5A-B). Of the distal projections, the projections to the SN and MRN were the densest on average (Figure 5B).

In order to test if this population was the critical source of local dynorphin for CeA KOR-mediated effects on anxiety and threat discrimination, we selectively reduced CeA dynorphin expression by injecting AAV1-Cre-GFP bilaterally into the CeA of *Pdyn*$^{lox/lox}$ animals (Pdyn KO) (Figure 5C). Genetic inactivation of Pdyn in the CeA resulted in a significant reduction of *Pdyn*$^{+}$ cells (Figure 5D). Pdyn KO animals showed no significant differences compared to controls on the elevated plus maze, with no differences in time spent in open or closed arms or latency to enter the open arm before or after fear conditioning (Figure 5F-G, latency data not shown). There were also no differences in post-fear conditioning anxiety (Figure 5H). These animals were fear conditioned, with no significant alteration in shock response (Figure 5I) or fear acquisition during training (Figure 5J-M). Controls and KOs demonstrated significant fear expression during the post-conditioning probe, though KOs presented a mild non-significant decrease in average CS+ freezing compared to control CS+ freezing (Figure 5N-O). It was clear that local CeA Pdyn KO did not recapitulate the anxiety and fear generalization phenotype induced by CeA KOR KO. Thus, we hypothesized that there were other non-local sources of dynorphin in the CeA.

Figure 5

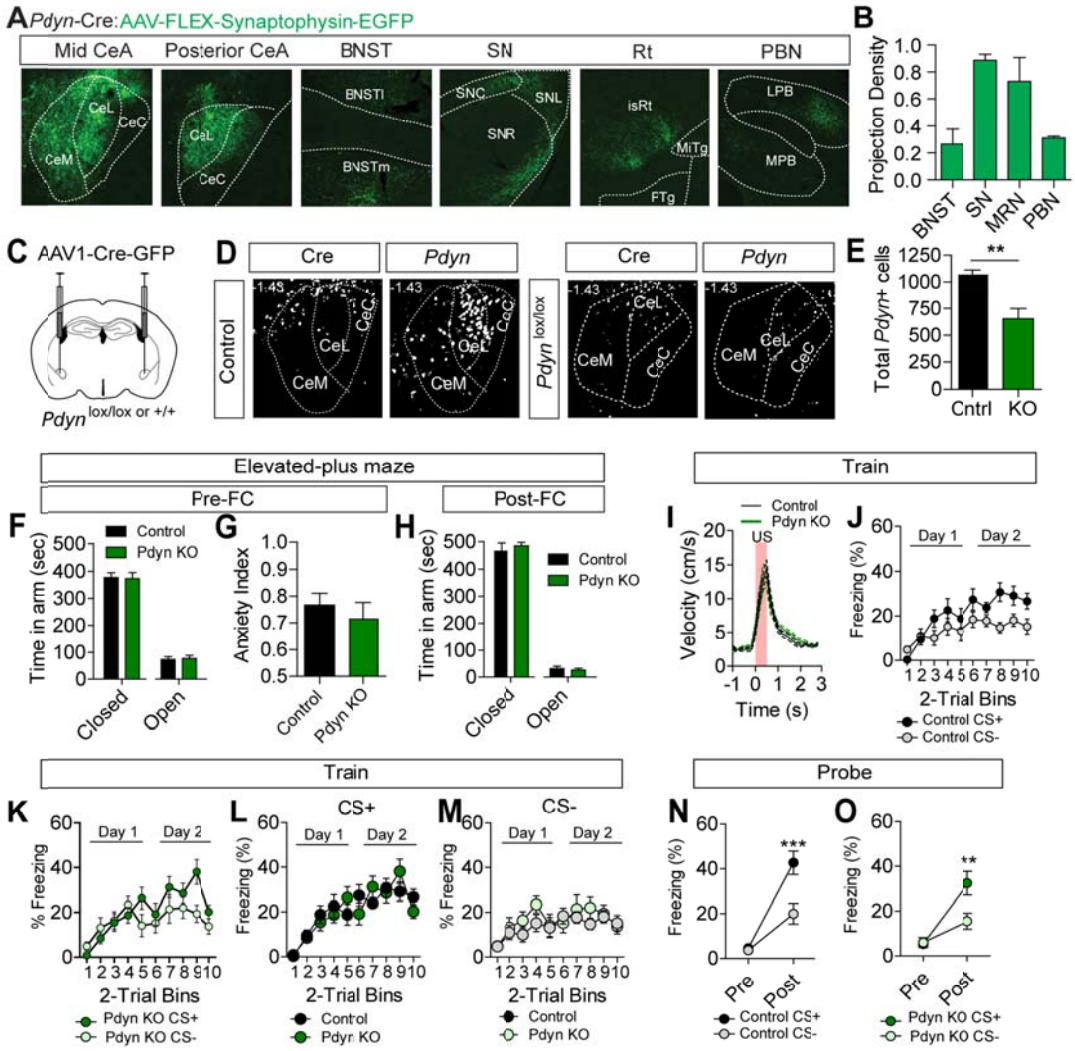

Figure 5: CeA dynorphin (Pdyn) knockout has no effect on anxiety or fear learning

(A-B) AAV1-Synaptophysin-EGFP was injected unilaterally into the CeA of *Pdyn*-Cre animals to visualize CeA *Pdyn*+ projections. Dense projections were visualized locally throughout the CeA as well as distally in the bed nucleus of the stria terminals (BNST), substantia nigra (SN), reticular thalamus (Rt), and parabrachial nucleus (PBN). Distal projections (which did not have cell bodies confounding quantification of EGFP tagged terminals) were quantified. Pixel density is calculated as (RawIntDen (sum of the values of the pixels) / area). Normalized density= Pixel density/max pixel density. (n=2-3) (One-way ANOVA $F(3,6)=5.068$, $^{*}p<0.05$; Turkey's multiple comparisons test. n.s. $p>0.05$).

(C) Schematic of AAV1-Cre-GFP bilateral injection into the CeA of $Pdyn^{lox/lox}$ mice (Pdyn KO) or wild type (control) mice.

(D-E) Example in situ hybridization shows Cre and *Pdyn* expression in the CeA, and a significant reduction in *Pdyn*+ cells (n=3-5 injections) (unpaired t-test, $^{**}P<0.001$), resulting in a 40% knockout of CeA *Pdyn*. Quantification is from six sections from -1.19 to -1.79cm from Bregma.

(F-H) CeA Pdyn KO had no effect on anxiety measures in the elevated plus maze pre or post fear conditioning. Pdyn KO animals spent the same amount of time in the open and closed arms as controls, and had no change in their anxiety index (n=17-20) (unpaired t-test, $P>0.05$).

Both groups spend more time in the closed arm after fear conditioning with no difference between groups.

(I) Velocity in reponse to foot shock was not altered by Pdyn KO during the 0.5-sec footshock or the two seconds after shock onset (Two-way ANOVA $p>0.05$).

(J-M) Control and Pdyn KO animals increased freezing to the cues throughout two-day-shock training (Two-way ANOVA, effect of time, $^{***}P<0.001$). Acquisition of CS+ and CS- freezing was not significantly different between groups over the two days (Two-way ANOVA, $P>0.05$).

(N-O) Control and Pdyn KO animals show increased freezing to the cues after shock-training (Two-way ANOVA, $^{**}P<0.01$, effect of time $^{***}p<0.001$), and both groups discriminate between CS+ and CS- cues (two-way ANOVA, bonferroni post test $^{***}p<0.001$, $^{**}p<0.01$). Pdyn KO animals showed a non-significant trend toward decreased freezing to the CS+ compared to controls (unpaired t-test, n.s. $P=0.18$) (n=17-20 for all anxiety and fear conditioning).

To investigate distal sources of dynorphin projecting to the CeA, we injected a Cre-inducible retrograde virus Retro-AAV2-FLEX-GFP unilaterally into the CeA of *Pdyn*-Cre animals (Figure 6A). This retrograde virus transduces CeA-targeting *Pdyn*-expressing cells by infecting their terminals and utilizing axonal transport to traffic the plasmid to the cell body [64]. Locally, the injection labeled cells throughout the entire anterior-posterior axis of the CeA (Figure 6B) as well as a minority of caudate putamen cells, dorsal to the CeA (examples of individual viral spread in Figure 6E). Retrogradely labeled cells were found from +3 mm to -4.7 mm from bregma, mostly in cortical and hypothalamic regions. The regions with the most cells labeled were the cingulate, insular, entorhinal, and visual cortices (Figure 6C,F).

Given that CeA *Pdyn* KO did not induce anxiety and fear generalization, we decided to test whether KO of all sources of dynorphin to the CeA would result in a similar behavioral phenotype to CeA KOR KO. If so, then it is possible that this phenotype is dependent on dynorphin released into the CeA acting on locally expressed CeA KOR. If KO of all sources of dynorphin to the CeA does not recapitulate KOR KO phenotypes, then the effect of KOR KO might be due to KOR expression on terminals outside of the CeA. Another explanation is that there may be an additional ligand of CeA KOR mediating this effect that is not expressed by the *Pdyn* gene, though this would be unlikely.

To test the hypothesis, we knocked out all sources of dynorphin to the CeA using a retrograde CAV2-Cre virus injected bilaterally into the CeA of $Pdyn^{lox/lox}$ animals (Figure 7A). CeA targeting was visualized using AAV1-FLEX-GFP, which was co-injected with CAV2-Cre. On the elevated plus maze, CAV *Pdyn* KO (CAV KO) animals showed increased time in the closed arms and a strong trend towards a reduction in time spent in the open arm (Figure 7B), which resulted in a significant increase in anxiety score (Figure 7C). Both CAV KO and control animals displayed non-significantly different high-anxiety behavior after shock training (Figure 7D), but CAV KO animals showed a trend toward a longer latency to enter the open arm ($p=0.10$) (data not shown).

During fear conditioning, CAV KOs displayed normal fear acquisition and response to shock (Figure 7E-G). Unlike controls though, during the post-conditioning probe trial CAV KO animals displayed an increase freezing during the CS- tone, which resulted in reduction in cue discrimination between the CS+ and CS- (Figure 7H-K). Thus, retrograde KO of all sources of Pdyn to the CeA phenocopied the CeA

KOR KO increases in anxiety and decreases in fear discrimination. This suggests that this effect on anxiety and fear discrimination is likely dependent on distal dynorphin projecting into the CeA and acting on KOR expressed locally in the CeA.

Figure 6

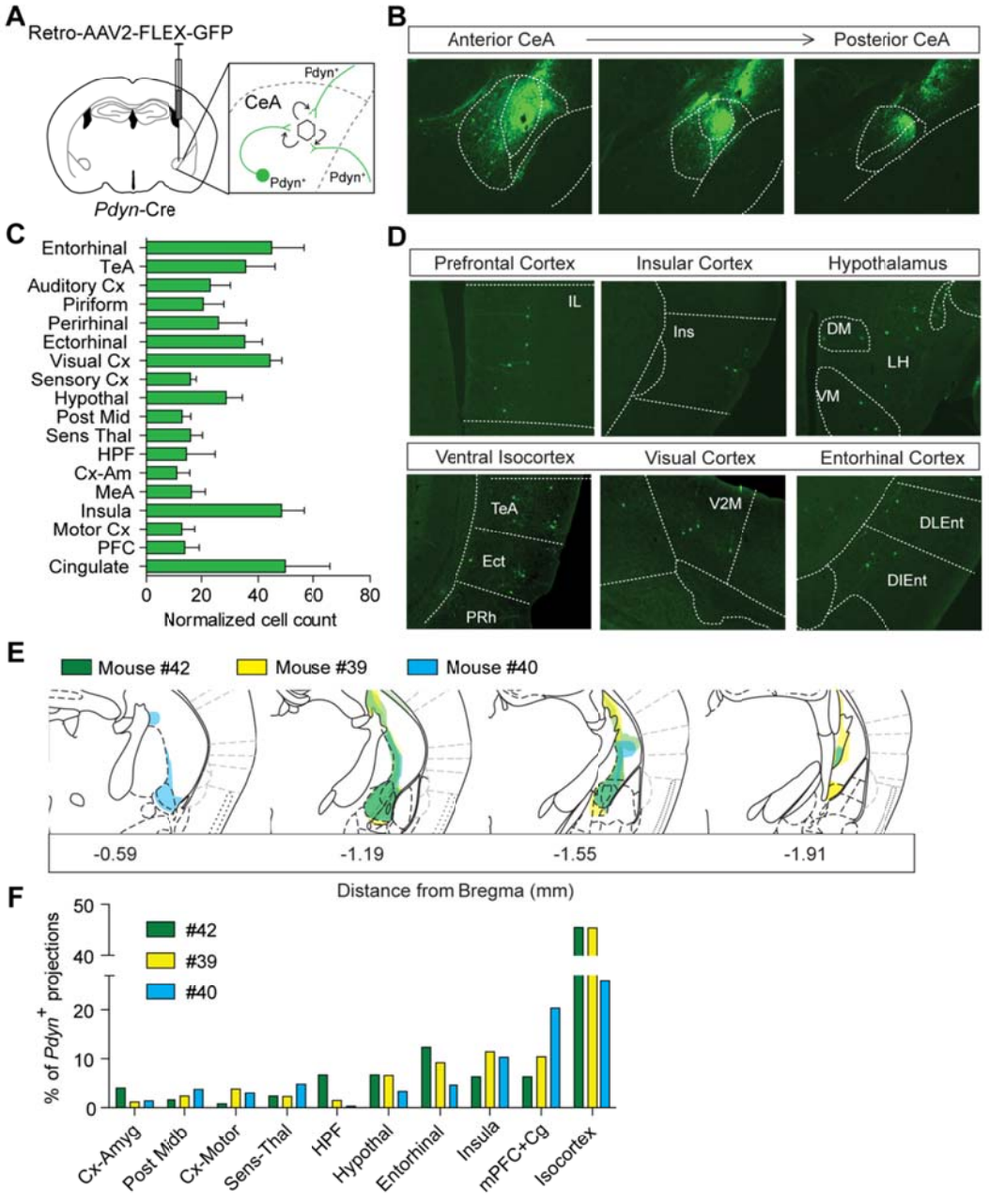

Figure 6: *Pdyn*+ cells from all over the brain project to the CeA
(A) Schematic for unilateral injection of retrograde AAV2-FLEX-GFP into the CeA.
(B) Local CeA targeting of Pdyn+ cells
(C-D) Brain-wide retrograde labeling of Pdyn+ cells projecting to the CeA. Abbreviations: temporal association cortex (TeA), cortex (Cx), hypothalamus (hypothal), midbrain (Mid), sens thal (sensory thalamus), hippocampal formation (HPF), cortex-amygdala transition zone (Cx-Am), medial amygdala (MeA), prefrontal cortex (PFC). (n=3). Normalized cell count is calculated as (region cell count)/(mouse total/average total)
(E-F) Individual targeting and retrograde labeling quantification.

Figure 7

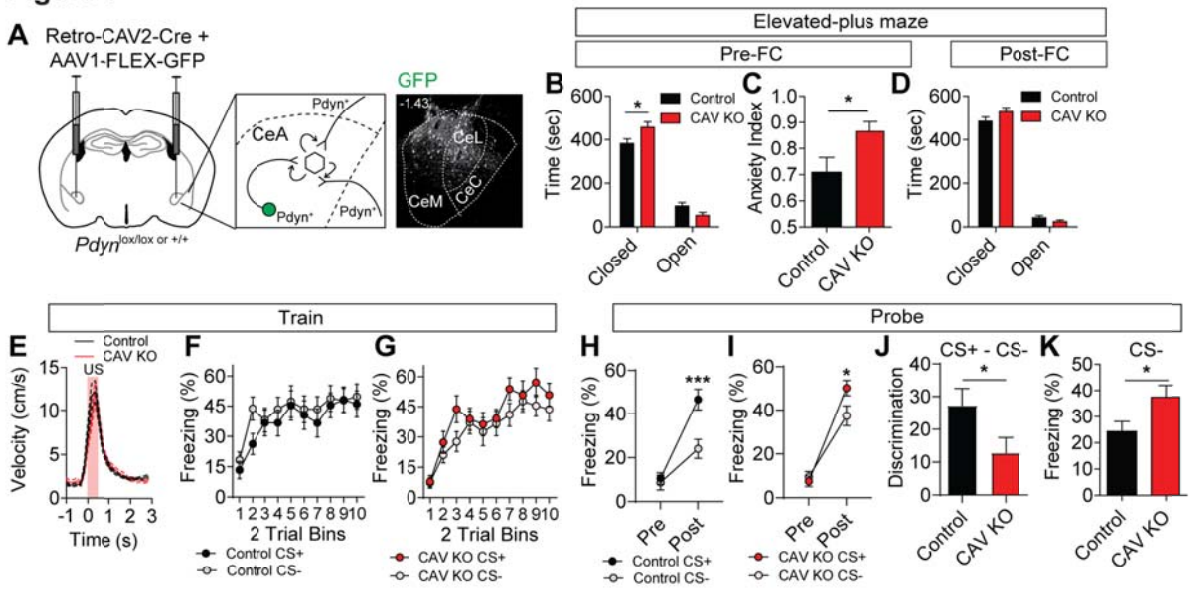

Figure 7: Knockout of all sources of dynorphin to the CeA replicates CeA KOR KO with increases in anxiety and fear generalization
(A) CAV2-Cre + AAV1-FLEX-GFP was injected into the CeA of *Pdyn*$^{lox/lox}$ mice (CAV KO) or wild type (control) mice. CeA targeting was verified with local GFP expression.
(B-D) CAV Pdyn KO animals spent increased time in the closed arms of the maze (n=11-15) (unpaired t-test **P<0.01) and showed an increase in their anxiety index, which is calculated as 1- ((open arm time)/(closed arm time)) (unpaired t-test *P<0.05). 3 days post-fear conditoning, animals show increased time in the closed arm compared to pre-condiitoning (unpaired t-test **p<0.01 for controls, *p<0.05 for mutants), but are no longer significantly different between groups.
(E) Velocity in reponse to foot shock was not altered by CAV Pdyn KO during the 0.5 sec footshock or the two seconds after shock onset (Two-way ANOVA p>0.05).
(F-G) Control and CAV Pdyn KO animals increased freezing to the cues throughout two day shock training (Two-way ANOVA, effect of time, ***P<0.001). Acquisition of CS+/- freezing was unchanged (Two-way ANOVA, effect of genotype, p>0.05)
(H-I) : Control and KOR KO both show increased freezing to the cues after shock training (Two-way ANOVA, effect of time ***p<0.001), and both groups display some degree of discrimination (Two-way ANOVA, bonferroni post test ***p<0.001, *p<0.05).
(J-K) CAV Pdyn KO animals had a significant reduction in their post training discrimination score (CS+ - CS-) (unpaired t-test *p<0.05) due to an increase in CS- freezing (unpaired t-test *p<0.05) (n=15-17 for all training and probe).

Pharmacological inhibition of CeA KOR

Our findings suggest that a reduction of KOR-expression in CeA cells results in non-cue-specific fear-learning. This genetic manipulation results in genetic knockout of *Oprk1* in cells with cell bodies in the CeA, and on terminals of CeA cells that have both local and distal projections (Figure 8A). This differs from pharmacological approaches such as antagonist infusion into the CeA, which inhibits KOR expressed on cell bodies and terminals local in the CeA. This approach does not specifically target cells with cell bodies in the CeA, and can target terminals projecting into the CeA (Figure 8A). Thus, pharmacological and genetic approaches target different populations of KOR.

Given that another group has shown that pharmacological inhibition of KOR in the CeA results in reductions in associative fear learning using a fear potentiated startle assay [40], we were interested to see whether targeting this slightly different KOR population would result in reductions in fear learning or dysregulated generalized fear. The long-acting KOR antagonist, NorBNI, was infused bilaterally into the CeA 24 hours before the start of day 1 of fear conditioning (Figure 8B). NorBNI did not alter physical response to shock (Figure 8C) and NorBNI-treated animals display normal fear acquisition during shock training (Figure 8D). During the post-conditioning probe trial, though, while controls exhibited discriminative fear, NorBNI animals did not significantly discriminate between the CS+ and CS- (Figure 8E-F). This lack of discrimination was due to a trend in reduced CS+ freezing, which was not significantly lower than controls (Figure 8G). NorBNI-infused animals also showed a strong trend toward reduced CS+ - CS- discrimination, which was not significant (Figure 8H), likely due to a large amount of variation in these cannulated animals.

While pharmacological block also results in a lack of cue discrimination, this phenotype is different than the virally-induced KOR KO, as the effect is largely carried by a decrease in CS+ freezing. NorBNI-infused animals still display significant learning during the post-conditioning probe, but that learned fear is non-significantly reduced and non-cue specific.

Figure 8

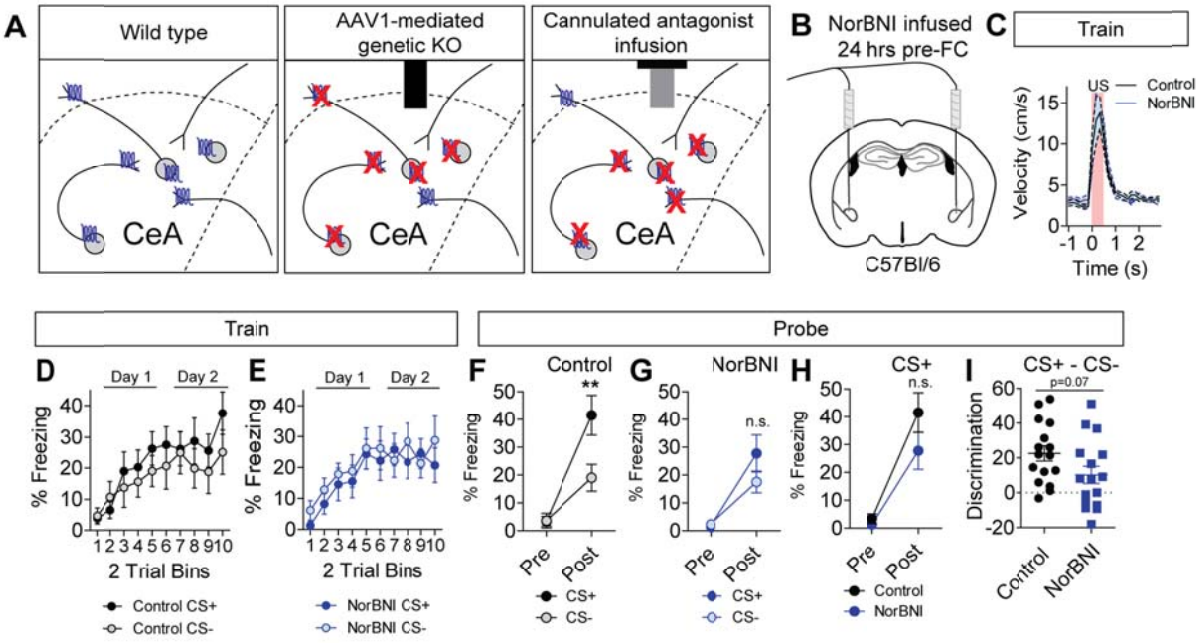

Figure 8: CeA KOR antagonism disrupts discriminative fear learning
(A) Example images of KOR populations targeted with CeA-targeting virally-transduced genetic knockout versus CeA-targeted cannulated drug infusion.
(B) NorBNI was bilaterlaly infused in the CeA using implanted cannulae 24 hours pre-fear conditioning (FC) day 1.
(C) Velocity in reponse to foot shock was not altered by NorBNI, 24 hours after infusion, during the 0.5 sec footshock or the two seconds after shock onset (Two-way ANOVA $p>0.05$).
(D-E) Control and NorBNI animals increased freezing to the cues throughout two day shock training (Two-way ANOVA, effect of time, $^{***}P<0.001$). Acquisition of CS+/- freezing was unchanged (Two-way ANOVA, effect of genotype, $p>0.05$)
(F-G) : Control and KOR KO both show increased freezing to the cues after shock training (Two-way ANOVA, effect of time $^{***}p<0.001$), and both groups display some degree of discrimination (two-way ANOVA, bonferroni post test $^{***}p<0.001$, $^{*}p<0.05$).
(J-K) CAV Pdyn KO animals had a significant reduction in their post training discrimination score (CS+ - CS-) (unpaired t-test $^{*}p<0.05$) due to an increase in CS- freezing (unpaired t-test $^{*}p<0.05$) (n=15-17 for all training and probe).

Discussion: CeA KOR is necessary for normal anxiety and discriminative fear learning

It has been well established that dynorphin and KOR play a critical role in response to stress and that the net effect of global KOR activation is dysphoria and anxiety [45, 65-67]. This has led to the generalization that dynorphin acts as pro-stress molecule in all circuits, when the reality is more complex. Acute stress-induced KOR activation also results in a variety of adaptive responses to threat. KOR activation results in analgesia, which increases an organism's ability to escape danger. KOR-mediated dysphoria and aversion, associated with a stress-inducing threat, motivates the organism to engage in behaviors to avoid the hazard in the future [48]. Dynorphin is a signaling peptide without an innate valence and its

effects are entirely dependent on the localization of its inhibitory receptor, KOR. Here in the CeA, KOR activation appears to be necessary for stress reduction and cue discrimination during a threat.

There were hints that CeA KOR would play a role in reducing anxiety and associated fear over-generalization. An electrophysiology study reported that KOR may have opposing effects on physiology in the CeA compared to CeA CRH, which is known to enhance fear [39, 68, 69], [58]. The location of KOR expression also suggests a role in inhibiting cells which elicit fear behaviors. Our work revealed that KOR is expressed largely in the CeL and CeM subdivisions. Our RiboTag and in situ hybridization findings complement data showing that about 40% of CeL KOR overlaps with dynorphin [53], which labels the "fear on" freezing-inducing dynorphin^{+}; somatostatin^{+} population [13, 24, 25, 54]. KOR-mediated inhibition of the CeL "fear on" population in addition to CeM output neurons would reasonably lead to a decrease in overall CeA fear output signal.

We hypothesize that local KOR's effect on baseline anxiety was not previously identified [53] because singly housing animals results in a robust alterations in neural circuits and increases anxiety [70, 71]. Our animals are group housed and upon CeA KOR KO, animals displayed significant increases in anxiety compared to controls (Figure 4E-F). This significant difference on the EPM behavior is erased when animals are already stressed, such as after fear conditioning (Figure 4G).

A number of groups have studied the role of CeA-produced dynorphin in behavior and have found that it can modulate alcohol intake [42, 53, 72], though CeA dynorphin's role in other behaviors is less well understood. A recent publication demonstrated that *Pdyn* KO in CeA *Crh*$^{+}$ neurons in rats reduces freezing during probe trials [41], though we found that non-cell type specific CeA dynorphin KO in mice resulted only in a mild and non-significant decrease in CS+ freezing (Figure 7N-O). Both studies reported about a 40% reduction in *Pdyn* mRNA, though we used *in situ* analysis and *Pdyn*+ cell counting, while the other group used qPCR quantification of total mRNA levels. This difference in behavioral results could be due to the manipulation of slightly different dynorphin populations, differences in rat and mouse circuitry, or both. Regardless, it is clear that local CeA dynorphin KO does not phenocopy CeA KOR KO, and that a distal source of dynorphin projects onto CeA KOR, maintaining normal baseline anxiety and fear discrimination. Our retrograde tracing suggests that this critical source of dynorphin could be cortical or

hypothalamic, but the wide dispersion of CeA-projecting *Pdyn*$^{+}$ cells makes it difficult to specifically target and test individual populations. Further studies will need to investigate the role of *Pdyn*$^{+}$ projections to the CeA from the isocortex and hypothalamus, and their potential roles in CeA-associated behaviors. It is possible that release of dynorphin from a combination of some or all of these distal regions could be necessary for normal discriminative fear and anxiety behavior.

Our pharmacological blockade of KOR located in the CeA also resulted in cue generalization, but this was largely due to a trending decrease in CS+ freezing instead of a trending increase in CS- freezing, as we observed with CeA KOR KO. Although these are both examples of a lack of cue discrimination, it is critical to note that one displays notably high CS- freezing while the other displays low CS+ freezing. In order to better understand this phenotype, future experiments could be performed where animals received NorBNI 24 hrs before anxiety assays. Due to reports that NorBNI effects on KOR-expressing terminals may reduce after one week, we performed the three days of fear conditioning 24 hours after NorBNI infusion. Thus, we avoided delaying fear experiments by an additional day by forgoing pre-fear-conditioning anxiety testing. If NorBNI infusion does not increase anxiety, this might suggest that NorBNI and KOR KO result in slightly different phenotypes, both of which include a lack of cue discrimination. Additionally, it is hard to interpret these pharmacological findings, as fear conditioning results were highly variable between cohorts. This might be due to spread of the drug outside of the CeA in some animals.

The report that CeA KOR opposes of CRH synaptic effects [58] seems counterintuitive, as both CRH and dynorphin have been implicated in CeA-mediated fear responses, and dynorphin has been shown to be necessary for global CRH-mediated stress effects. It is possible that CRH and dynorphin may have opposing behavioral actions specifically in the CeA, but it is also feasible that dynorphin's negative modulation of CRH-synaptic effects may be required for normal CRH-mediated fear learning. CRH-elicited increases in extracellular CeA dynorphin [62] might be acting as a negative feedback mechanism, providing a necessary control curtailing the effects of CRH release in a timely fashion. Thus, we hypothesize that normal discriminatory fear-learning relies on both CRH stimulation of CeA cells and then inhibition via dynorphin release and activation of CeA KORs. It is clear that further study is needed to understand CeA KOR circuitry and its role in fear learning. A better understanding of this pathway, how it

interacts with CeA CRH, and the role of these peptides in the modulation of discriminative versus generalized fear could aid in the discovery of new drug targets for the treatment of fear and anxiety disorders.

Part IV: Dopamine inputs to the CeA and their role in discriminative fear

Dopamine and cue discrimination

The CeA acts as a hub of threat information. It regulates threat responses, determining whether an organism's response is discriminative for known threats, or generalized to a wider range of related cues. Threat discrimination is a complicated calculation which involves both perception of threat intensity and generation of a correct defensive responses based on the perceived degree of threat. This complex response relies on a coordination of neuropeptide and other neuromodulator signaling systems to carefully tune responses to varied levels of perceived threats. Thus, we wanted to interrogate other modulators of CeA signaling which play a critical role in fear discrimination.

The CeA directly receives cue information from a variety of extra-amygdalar neuromodulatory systems, including midbrain dopamine neurons [33]. The ventral tegmantal area (VTA) in the midbrain is a well characterized population of dopamine neurons that plays a critical role in signaling cue information such as its degree of importance, or salience, and whether the cue has a positive or negative association, or valence [73]. It is well established that dopamine plays a critical role in fear learning [74, 75]. Additionally, dopamine inputs to the CeA and CeA dopamine receptors have been demonstrated to play a critical role in discriminative fear learning. Knockout of dopamine neuron NMDA receptor (NR1, encoded by *Grin1*) signaling and LTP [76], or blocking dopamine receptor 2 (D2, *Drd2* gene) signaling in the CeA [37] results in fear generalization. Stimulation of dopamine transporter (DAT, *Slc6a3* gene) expressing projections to the CeA increases cue discrimination at high threat intensities, where controls display cue generalization [36]. These findings suggest a critical role of dopamine cells in threat discrimination, but the critical signaling molecule and dopamine population within the midbrain had yet to be identified.

VTA dopamine neurons project to the CeA, and have been shown to release dopamine, glutamate, as well as peptides [33, 77], so the molecule(s) responsible for stimulation-induced discrimination is unknown. Additionally, phenotypes based on CeA dopamine receptor antagonism could depend on dopamine input from a variety of sources including the VTA, substantia nigra (SN), the ventral periaquiductal gray (PAG), and the dorsal raphe (DR) [78, 79]. We aimed to characterize dopamine inputs

to the CeA and their role in discriminative fear in order to better elucidate discrimination-inducing CeA circuits.

Characterization of midbrain to CeA inputs mediating cue discrimination

First, we wanted to identify sources of dopamine that project to the CeA. We used floxed-stop tdTomato (*Rosa26*$^{fs\text{-}tdTomato}$, or *Rosa26*^{Ai14}) mice, that express the tdTomato fluorophore in a Cre-dependent manner. Retrograde CAV2-Cre was injected into the CeA and brain sections containing the dopamine-expressing VTA, SN, and DR were collected. Next, we stained for tyrosine hydroxylase (TH) which identifies midbrain dopamine and locus coeruleus norepinephrine neurons. Dopamine cells which send projections to the CeA were identified by tdTomato$^+$ and TH$^+$ coexpression in regions known to express dopamine, but not NE. CeA projecting TH$^+$ cells were identified in the VTA, the SN, and the dorsal and caudal linear raphe (DR/CLI), suggesting that CeA dopamine may originate from any of these three regions (Figure 9A).

Extracellular dopamine increases in the amygdala during aversive learning, and active avoidance requires dopamine release in the amygdala [80]. To determine which of these three regions are involved in dopamine release into the CeA in response to threats, we examined Fos, encoded by the immediate early gene *Fos*, and TH protein expression after 0.3-mA shock training. Mice underwent fear conditioning to a low intensity 0.3-mA foot shock, then 90 minutes after conditioning, brains were collected. Fos$^+$/TH$^+$ cells are presumably dopamine cells that were strongly activated during conditioning. We identified these shock-training-activated TH$^+$ cells in the VTA and the raphe, but not in the SN (Figure 9B-C). This result suggests that dopamine cells the VTA and DR/CLI, but not the SN, are responsive to threat learning. There were significantly more activated dopamine cells in the VTA than the DR/CLI, suggesting that the VTA could be the critical source of dopamine to the CeA during aversive learning.

Previous work from our lab has demonstrated that stimulation of VTA dopamine projections to the CeA enhances cue discrimination, and inhibition of these projections causes an increase in generalization [36]. To investigate the dopamine dependence of this effect, we conditioned animals with a 0.5-mA high-threat-intensity foot shock, which induces generalization in controls. During conditioning, we stimulated

VTA→CeA projections with channel rhodopsin (ChR2) with or without projection-specific knockout of dopamine. This was accomplished using wild type and $TH^{lox/lox}$ animals. We injected CAV2-Cre bilaterally into the CeA and AAV1-FLEX-ChR2-mCherry or AAV1-FLEX-mCherry unilaterally into the VTA, with an optic fiber implanted above the VTA (Figure 10A). Stimulation of all VTA projections to the CeA resulted in increased cue discrimination. Animals with the projection-specific dopamine KO, though, had significantly lower discrimination than stimulation alone (Figure 10B-C). Thus, the VTA projections to the CeA that increase discrimination require dopamine expression.

Figure 9

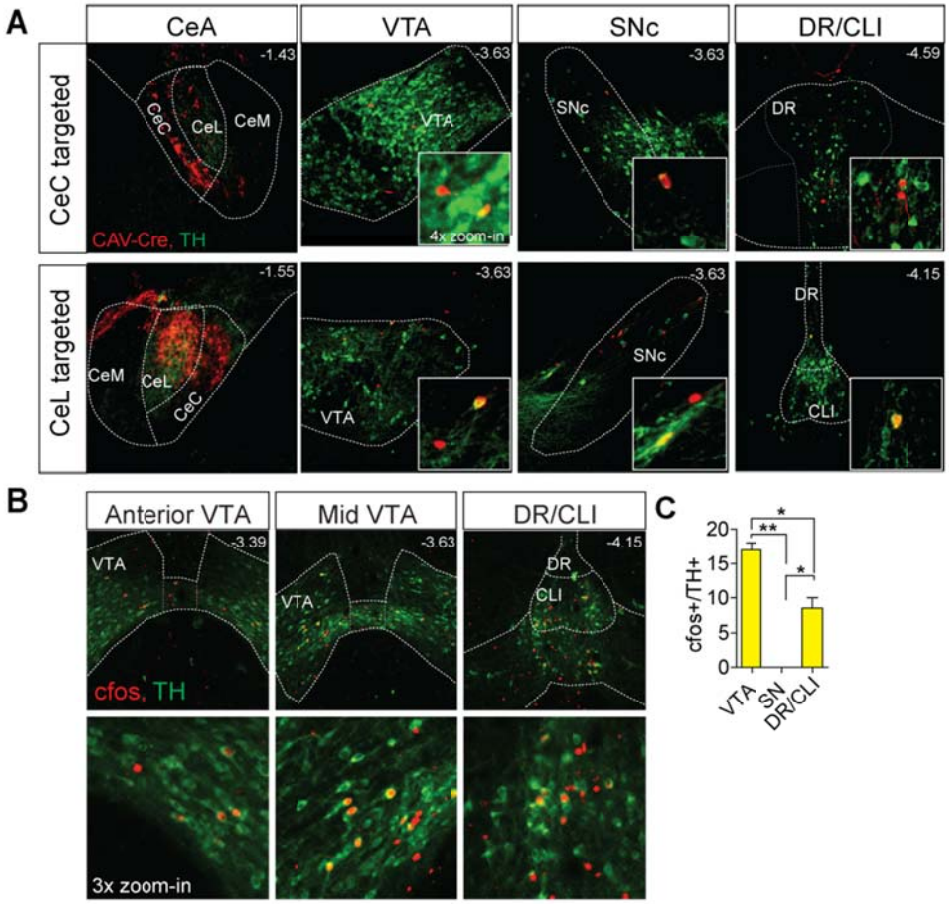

Figure 9: Dopamine cells project to the CeA and are activated by shock training
(A) CAV2-Cre was injected into the CeA of flox-stop tdTomato animals. Cre-activated Tomato is in red and tyrosine hydroxylaze (TH) is in green. Injections targeting the CeC and the CeL retrogradely labeled TH+ dopamine cells in the ventral tegmental area (VTA), substantia nigra compact part (SNc), and the raphe dorsal and caudal linear nuclei (DR and CLI). Insets are 4x zoom-in images.
(B) Example images of dopamine cells activated by 10x 0.3mA shock training. cFos is in red and TH in green. 3x zoom-in below.
(C) Number of cells coexpressing cfos and TH was quantified in the VTA, SN, and raphe (DR/CLI) (n=2) (One-way ANOVA $F(2,3) = 66.69$, $^{**}p<0.01$; Turkey's multiple comparisons test, $^{**}p<0.01$, $^{*}p<0.05$).

Figure 10

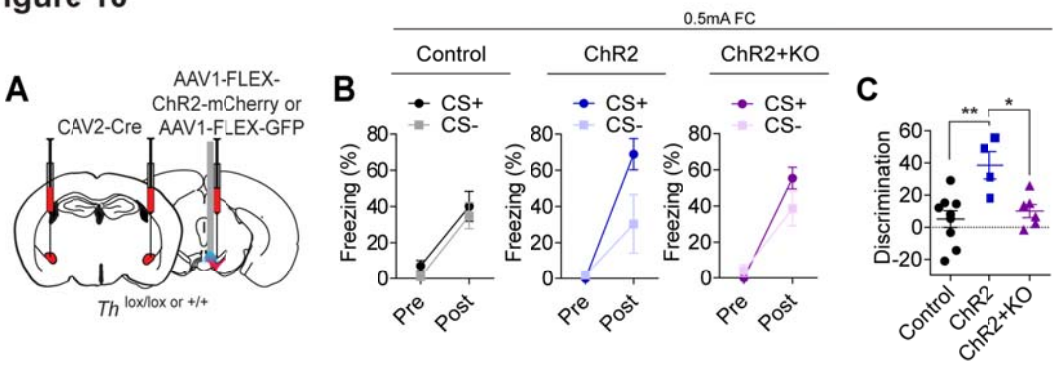

Figure 10: Dopamine knockout from VTA projections to the CeA blocks VTA to CeA induced discrimination
(A) Schematic of surgical procedures. CAV2-Cre was injected into the CeA bilaterally for all groups. Channel rhodopsin stimulation (ChR2, $TH^{+/+}$) and stimulation + knockout (ChR2+KO, $Th^{lox/lox}$) mutants received AAV1-FLEX-ChR2-mCherry unilaterally in the VTA with an optic fiber. Controls (+/+) received AAV1-FLEX-GFP and an optic fiber into the VTA.
(B) Animals were fear conditioned with a 0.5-mA foot shock which induces generalized fear in controls. Pre and post shock training probe trials are shown. Control and ChR2+KO animals displayed clear cue generalization (Two-way ANOVA, effect of treatment p=0.311 and p=0.284 respectively). ChR2 animals trended toward cue discrimination (Two-way ANOVA, effect of treatment p=0.083).
(C) Discrimination scores are calculated as freezing (%) to the CS+ minus the CS-. Controls and ChR2+KO animals no not discriminate, as their discrimination scores are not significantly different from zero, but ChR2 animals significantly discriminate (One sample t-test compared to a theoretical mean= 0, controls and ChR2+KO p>0.05, ChR2 *p<0.05). Stimulation only animals (ChR2) had significantly greater discrimination than control and ChR2+KO groups (One-way ANOVA **p<0.01; Turkey's multiple comparisons test, **p<0.01, *p<0.05) (n=4-9).

Discussion: VTA and raphe dopamine likely mediate cue discrimination

To understand circuitry underlying fear discrimination, we aimed to further elucidate the dopamine projections to the central amygdala. Dopamine cells from a variety of regions project to the CeA. VTA and raphe dopamine populations, though, are most likely to be critical for fear discrimination as they are activated in response to fear conditioning. Additionally, we identified that dopamine is a critical mediator of VTA→CeA mediated discrimination. We demonstrated that stimulation of CeA projecting VTA cells only increases discrimination when they express *Th*. These findings further support that the release of dopamine into the CeA from the VTA is a critical circuit for cue discrimination. This further supports the theory that VTA dopamine is critical for processing cue salience and valence [73].

Future directions include a better understanding of which dopamine subpopulations are critical mediators of discrimination. The CAV-Cre activated tdTomato and Fos study suggests that only a small population of VTA cells activated by threat project to the CeA. It is unknown whether the CeA-projecting population mediating fear discrimination is localized in a particular subregion of the VTA or expresses particular

genes. Additionally, it is important to note that the CAV2-Cre retrograde knockout of TH results in a decrease in both midbrain dopamine and locus coeruleus norepinephrine in cells which project to the CeA. In the future, this experiment could be improved to only target midbrain dopamine by using all wild type animals, and injecting a Cre-dependent CRISPR virus targeting TH into the VTA to induce projection-specific knockout.

V. Dissertation final summary and discussion

It is clear that the perception of and response to perceived threats rely on a variety of circuits and signaling molecules. Our previously published work has identified CeA CRH-CRHR1 as a critical signaling system specifically for cue-specific discriminative fear [39] .Now we have demonstrated that normal discriminative fear learning is dependent on CeA KOR as well as dynorphin and VTA dopamine inputs to the CeA.

Progress will ultimately be made in treating generalized fear disorders once we gain an understanding of how these various signaling systems work together to produce fear output. Tools such as chimeric-GPCR fluorescent sensors, which are activated in response to particular neuropeptide or neuromodulator binding [81, 82], could be used to measure temporal release of dynorphin, CRH, and dopamine in the CeA. Additionally, they could be used to inform how peptide release in the CeA can change in disordered states. A better understanding of how these critical circuits cooperate to mediate appropriate discriminative fear responses would propel the field of fear research, and provide new insights for the treatment of generalized fear and anxiety disorders.

The potential of for using KOR-modulating drugs for treatment of anxiety disorders is complicated. Our findings identify that KOR expressed in the CeA is a critical for promoting discriminative fear and normal low baseline anxiety. This is very different than the role of global KOR, or even KOR in the BLA [49, 59, 83], which is largely anxiogenic and dysphoric upon activation. Additionally, it has been shown that global activation of KOR with U50 can actually increase cued fear renewal [59], which is the opposite of what we would want for the treatment of anxiety and PTSD patients. Thus, any treatment option aimed at reducing fear generalization and anxiety would likely require very specific targeting of CeA KOR. This would be possible if region-specific binding partners of KOR were identified so that a treatment could target these binding partners and indirectly modulate KOR activity specifically in the CeA. Identification of these molecules would be possible using SILAC-based mass spectrometry [84], and a comparison of KOR-associated proteins in the CeA versus the rest of the brain. Additionally, another possible drug target would include effecter molecules which mediate KOR signaling in the CeA more so than other brain

regions. These could include specific subunits of potassium channels which may play a more critical role in CeA signaling than other regions which mediate KOR's pro-anxiety and dysphonic phenotypes.

Our findings examine the role of CeA KOR and dopamine inputs to the CeA in the formation and acute expression of fear memories. This is useful for understanding fear circuitry and potential circuit changes that can lead to disordered generalized fear. Our work does not begin to assess the role of CeA KOR or dopamine in fear extinction and renewal, which are critical treatment points for patients with fear disorders. In order to better understand how CeA KOR could be a target for treating patients with fear and anxiety disorders, future directions should include experiments assessing whether CeA KOR manipulation could either enhance fear extinction or decrease cued fear renewal. This could be done by fear conditioning followed by genetic knockout, before extinction and retrieval trials. Drug infusion could also be used after fear conditioning, but as discussed above, drug infusion into the CeA also interacts with terminals targeting the CeA and can lead to different results. Additionally, experiments should be performed to see if activation of CeA KOR can reduce fear generalization or anxiety. Our work has demonstrated that CeA KOR is necessary to maintain a lower anxiety state, but we have not yet shown that CeA KOR is sufficient for lowering anxiety and blocking cue generalization.

Current FDA-approved first-line treatments for PTSD are largely limited to selective serotonin reuptake inhibitors [85], which are not efficacious in all patients. Treatments for PTSD targeting stress-associated neuropeptide receptors have been largely unsuccessful thus far. Treatments that have shown to be largely ineffective in clinical trials include CRHR1, neurokinin 1 receptor, and cholecystokinin receptor antagonists [86]. Thus, global alterations in neuropeptide signaling seem to be a less-promising route of PTSD-related drug discovery. It seems that more creative and specific treatments may be required, in addition to psychotherapy. It is possible that region-specific targeted manipulation of neuropeptide receptor signaling, such as activation of CeA KOR, may prove to be a more effective for the successful treatment of patients with PTSD.

Methods

Mice

Male and female *Pdyn*^{Cre}, *Oprk1*^{Cre}, *Pdyn*$^{lox/lox}$, *Oprk1*$^{lox/lox}$, and wild type mice on a C57BL/6 background were group-housed on a 12 h light/dark cycle with free access to food and water. Behavioral experiments were conducted during the light cycle (lights on at 7 am). All procedures were approved by the University of Washington Animal Care and Use Committee. Males and females were distributed evenly between groups.

Virus production and surgery

AAV1-FLEX-Synaptophysin-GFP, AAV1-Cre-GFP, AAV1-FLEX-Mcherry, AAV1-ChR2-mCherry, and CAV2-Cre produced in house (titer ~3×10^{12} particles/µl) as described [39, 69, 87]. AAV2retro-FLEX-EYFP was produced by the Washington University in St. Louis Hope Center, and was a gift from Dr. Michael Bruchas. Viral vectors were stored at −80 °C before surgery, and kept on ice on surgery day. Viral vectors were stereotaxically injected (0.5 µl) at a rate of 0.25 µl/min bilaterally into the CeA of isoflurane-anesthetized mice (2–4 months old) using the following coordinates: -1.165 mm posterior, ±2.91mm lateral, and either -4.6 or -4.7 ventral to bregma (according to the Paxinos atlas, average injection site was observed at -1.4 mm posterior of bregma) . All mice were allowed to recover from surgery for 2-3 weeks. All animals used for behavior underwent stringent histology checks to confirm that the virus displayed a bilateral CeA hit without targeting surrounding regions such as the basolateral amygdala or the caudate putamen. Extra-CeA targeting or low levels of viral expression in the CeA usually resulted in 30-50% of mutants' data being removed from experiments.

Cannulated drug infusions

For local infusions of NorBNI, mice were implanted bilaterally with a 4 mm guide cannulae above the CeA; infusion needles extended up to 1 mm below the cannulae. Recovery was allowed for 2 weeks after cannulae implants, prior to infusion. Bilateral NorBNI infusions occurred 24 hours before start of fear conditioning day 1. Animals were anesthisized with isoflurane and infused with 2.5µg of NorBNI bilaterally

into the CeA (5μg total, infusion per hemisphere: 0.5μL of 5mg/ml NorBNI in saline, infused over two minutes).

Anxiety: Elevated Plus Maze

Elevated Plus Maze (EPM) experiments were performed on a Med Associates EPM for mice (Product #: ENV-560A) which has two “closed arms” with black walls, two “open arms” with 1cm ledges, and white flooring. 10 minute sessions begin as the mouse is placed in a closed arm of the arena, with its nose at the edge of the center area boundary. Sessions were recorded from above and mouse center point movement tracked by Ethovision (Noldus) tracking software. Total distance traveled, time spent in open and closed arms, latency to enter the open arm, and frequency of open arm entries were analyzed. Frequency of open arm entries was highly variable and deemed unreliable, as the center point of animals standing at the edge of open arm often togged between the open arm and center area, creating an artificially high number of open arm entries. No significant differences were found in any experiment for distance traveled or latency to enter open arm but anxiety phenotypes could be observed through changes in open and closed arm time. Additionally, an “anxiety index” was calculated as 1-(open arm time/closed arm time), with a score of 1 showing maximal anxiety that can be detected by this behavioral paradigm.

Fear conditioning

Fear conditioning sessions were performed during the light cycle in a standard operant chamber (Med Associates Inc., VT) equipped with a house light, tone generator, and shock grid. Our discriminative, low-threat-intensity, fear-conditioning protocol is three days long and includes a baseline probe then shock training trial on day 1, an intermediate probe and second shock training trial on day 2, and a final probe on day 3.

During each training session, animals are exposed to 10 pairings of a CS+ auditory tone with a 0.3-mA US foot shock (or 0.5-mA foot shock, if specified), and 10 CS- tone presentations which are never paired with shock. Auditory CS cues included a 10 kHz pulsatile tone and a 20 kHz continuous tone, each 10 seconds in duration. The CS+ tone co-terminated with a 0.5-sec, 0.3-mA foot shock which began 9.5

seconds after the tone presentation began. Assignment of which tone would be the shock-paired CS+ or non-shock paired CS- was counterbalanced across groups. CS+ and CS- tone presentations alternated with a 60 second intertrial interval. The training context was all metal, with the shock grid floor, and the box was cleaned with 70% ethanol between trials.

Baseline and probe trials were run in a separate context, in an all white Med Associates box insert with a smooth floor that was cleaned with a 1% acetic acid between animals. The animals were exposed to alternating presentations of 3 CS+ and 3 CS- auditory tones (10 second tones as described above with a 60-second intertrial interval, but with no shock presentations). These trials were used to establish basal freezing to the tones on day 1 before shock training and to measure expression of learned fear of the tone(s).

All sessions were video recorded and nose, center, and tail points were tracked on each mouse using Ethovision (Noldus) tracking software. Velocities were calculated using an in house MATLAB (Mathworks) script, which calculates the animal's velocity given the movement of all three points. Freezing was defined as velocity <1 cm/sec that lasted ≥0.5 sec. "% Freezing" was calculated as the % of time during the 10-second CS tone that the animal was frozen. Probe trial % freezing was presented as an average response to the 3 CS+ tones and the 3 CS- tones for each experimental group during the day 1 baseline and the day 3 final probe. Training/acquisition freezing was presented as the 20 total CS+ or CS- trials, binned into an average of two trials (ex: average of trial 1 and 2, 3 and 4, etc.). To measure shock reactivity, the raw centerpoint velocity from Ethovision was graphed from 1 second before to 3 seconds after shock, for the first 10 shock trials.

Optogenetic stimulation

For optogenetic stimulation experiments, animals expressing channelrhodopsin (ChR2) were implanted with an optic fiber cannula 0.5mm dorsal to the injection site. The cannula was attached to the skull with Metabond and dental cement. Blue light lasers were adjusted to produce 15-mW power at the tip of the optic fiber under constant illumination. Stimulation occurred during fear training for 1 second at 20 Hz, starting concurrent with the onset of the CS+ auditory tone.

Histology and Immunostaining

Mice were anesthetized with 50mg/kg Beuthanasia-D and transcardially perfused with phosphate-buffered saline (PBS), followed by 4% paraformaldehyde until the tissue was firm. Whole brain tissue was dissected out and fixed overnight in 4% paraformaldehyde, and then cryoprotected by soaking in a 30% sucrose in PBS for 48 hours. The brains were frozen in OCT in a -20°C cryostat and then cryosectioned to produce 30-µm-thick sections. Brain sections of interest were collected in PBS with 0.1% sodium azide prior to immunostaining.

For whole brain retrograde labeling experiments, every section was collected and every third section was stained (approximately corresponding to one page in the Paxinos atlas), or every sixth for projection analysis. For CeA-specific immunostaining, sections were selected based on the Paxinos and Franklin reference atlas, selecting sections which cover the length of the CeA (y = -1.2 to -1.18.).

Selected sections to stain were washed in Tris-buffered saline (TBS) for 10 minutes then blocked in TBS + 0.3% TritonX 100 (TBST) +3% normal donkey serum (NDS) for 30 minutes. Then sections were incubated overnight in primary antibody diluted in TBST+NDS. Anti-GFP (polyclonal, 1:2000; Invitrogen A11122)(polyclonal, 1:1000, Abcam ab13970) was used to stain for GFP and eYFP tagged viruses and anti-dsRed (polyclonal, 1:2000; Clontech, 632496) was used for Mcherry-tagged viruses. Fos antibody (rabbit 1:2000, Milipore ABE457) was also used.

CeA Pdyn^{+} synaptophysin distal projections were quantified by collecting the whole brain then staining sections (for GFP, as described above) every 180um. Due to GFP expression in the cell bodies in the CeA, the density of projections in the CeA could not be quantified. Six extra-amygdalar projections were identified and quantified by drawing regions of interest (ROIs) around the target region. We measured the density of GFP-tagged projections by measuring the sum of the values of the pixels in the ROI (RawIntDen) and dividing that by the area of the ROI.

For the Pdyn^{+} retrograde projection labeling experiment, cells were counted throughout the whole brain. The location of labeled cells was determined using the Paxinos and Franklin mouse brain atlas.

Normalized cell count per region was calculated as [region count/ (mouse total labeled cells/ average total cells)].

RNAscope *in situ hybridization*

The RNAscope assay (Wang 2012) was performed on C57Bl/6 wild-type, and *Oprk1*$^{lox/lox}$, and *Pdyn*$^{lox/lox}$ adult mice. Viral vectors were injected (as described above) 2-3 weeks before brains were quickly excised, flash frozen in 2-methylbutane, and stored at −80°C. 20-μm brain slices were prepared spanning the CeA from -1.2 – 1.8mm posterior of Bregma (according to the Paxinos atlas). Sections were prepared for hybridization per manufacturer's (Advanced Cell Diagnostics, Inc) instructions using probes for *Cre* (Mm-*Cre*-*C2,* ACD Bio # 312281-C2), Pdyn (Mm-*Pdyn*-C3, ACD Bio # 318771), and *Oprk1* (Mm-*Oprk1*-C3, ACD bio # 316111-C2). Slides were coverslipped and imaged using Nikon Upright Widefield fluorescent microscope at 10x magnification. Analysis performed using ImageJ.

Paxinos and Franklin's mouse brain atlas [88] was used to determine CeA and subregion locations. Imaging exposure was chosen based on a reference area which did not receive Cre-GFP (the basolateral amygdala for *Oprk1*, and the caudate putamen for *Pdyn*). Expression in the CeA and knockout was measured as number of cells in the CeA expressing the gene of interest. Gene expression was quantified from y= -1.23 to -1.79 (atlas pages 41-46), and knockout was quantified over 5 sections from y=-1.31 to -1.79 for Oprk1 and 6 sections from y=-1.23 to -1.79 for Pdyn, based on location of gene expression. A cell was determined to express the gene of interest if there were 3+ transcript puncta associated with the same nucleus (visualized using DAPI Fluoromount-G). Cell counting and knockout quantification was performed for each unilateral injection. After noting differences in transcript expression level per cell between CeA subregions, we compared the density of transcript being expressed per subregion using Image J. Pixel density was calculated by measuring the sum of the values of the pixels in the ROI (RawIntDen) divided by the area of the ROI.

RiboTag

Brains were extracted and CeA punches were collected on ice. Brain tissue was homogenized and HA-tagged ribosomes containing actively translating RNA were collected using an anti-HA antibody coupled

to magnetic beads. Homogenates, HA-antibody, and magnetic beads were rotated overnight at 4°C. Cell-type specific RNA was eluted from the magnetic beads and isolated using an RNeasy micro kit (Qiagen). Total CeA RNA was isolated from homogenates using the RNAeasy micro kit without HA-antibody and magnetic bead steps. Total RNA was quantified using a RiboGreen RNA assay kit (invitrogen). cDNA was synthesized from RNA using Superscript IV (Invitrogen). Amount of RNA was quantified using qPCR.

Acknowledgements

Thank you to everyone who made this dissertation work possible. I would like to thank my labmates in the Zweifel lab for years of training and support. You all provided a wonderful work environment and community. Thank you to Christina Sanford and Bryan Gore for the technical mentorship and training when I first joined the lab. I have been lucky to work with some wonderful undergrads who have contributed to my dissertation work. Thank you to Phil Sim, TingTing Hsu, and Rachel Wang. Thank you to the Palmiter, Chavkin, Phillips, and McKnight labs for assistance and resources. Thank you to my committee for the insight and guidance on my project. Thank you to Larry Zweifel for resources and guidance, furthering both my project and my training as a neuroscientist. I am so thankful for the wonderful and supportive community I have found at UW.

References

1. Tovote, P., J.P. Fadok, and A. Luthi, *Neuronal circuits for fear and anxiety.* Nat Rev Neurosci, 2015. **16**(6): p. 317-31.
2. Rodrigues, S.M., J.E. LeDoux, and R.M. Sapolsky, *The influence of stress hormones on fear circuitry.* Annu Rev Neurosci, 2009. **32**: p. 289-313.
3. School, H.M., *National Comorbidity Survey (NCS).* 2007.
4. Davis, L., D.H. Barlow, and L. Smith, *Comorbidity and the treatment of principal anxiety disorders in a naturalistic sample.* Behav Ther, 2010. **41**(3): p. 296-305.
5. McSweeney, F.K. and E.S. Murphy, *The Wiley Blackwell handbook of operant and classical conditioning*. 2014, Chichester, West Sussex, UK: Wiley Blackwell. xxii, 738 pages.
6. LeDoux, J.E., *Emotion circuits in the brain.* Annu Rev Neurosci, 2000. **23**: p. 155-84.
7. Bailey, K.R. and J.N. Crawley, *Anxiety-Related Behaviors in Mice*, in *Methods of Behavior Analysis in Neuroscience*, nd and J.J. Buccafusco, Editors. 2009: Boca Raton (FL).
8. Aubry, A.V., P.A. Serrano, and N.S. Burghardt, *Molecular Mechanisms of Stress-Induced Increases in Fear Memory Consolidation within the Amygdala.* Front Behav Neurosci, 2016. **10**: p. 191.
9. McEwen, B.S., *Protection and damage from acute and chronic stress: allostasis and allostatic overload and relevance to the pathophysiology of psychiatric disorders.* Ann N Y Acad Sci, 2004. **1032**: p. 1-7.
10. Duvarci, S. and D. Pare, *Amygdala microcircuits controlling learned fear.* Neuron, 2014. **82**(5): p. 966-80.
11. Armony, J.L., et al., *An anatomically constrained neural network model of fear conditioning.* Behav Neurosci, 1995. **109**(2): p. 246-57.
12. Herry, C. and J.P. Johansen, *Encoding of fear learning and memory in distributed neuronal circuits.* Nat Neurosci, 2014. **17**(12): p. 1644-54.
13. Kim, J., et al., *Basolateral to Central Amygdala Neural Circuits for Appetitive Behaviors.* Neuron, 2017. **93**(6): p. 1464-1479 e5.
14. Han, S., et al., *Elucidating an Affective Pain Circuit that Creates a Threat Memory.* Cell, 2015. **162**(2): p. 363-374.
15. Keifer, O.P., Jr., et al., *The Physiology of Fear: Reconceptualizing the Role of the Central Amygdala in Fear Learning.* Physiology (Bethesda), 2015. **30**(5): p. 389-401.
16. Penzo, M.A., et al., *The paraventricular thalamus controls a central amygdala fear circuit.* Nature, 2015. **519**(7544): p. 455-9.
17. Bienkowski, M.S. and L. Rinaman, *Common and distinct neural inputs to the medial central nucleus of the amygdala and anterior ventrolateral bed nucleus of stria terminalis in rats.* Brain Struct Funct, 2013. **218**(1): p. 187-208.
18. Sarhan, M., M.J. Freund-Mercier, and P. Veinante, *Branching patterns of parabrachial neurons projecting to the central extended amgydala: single axonal reconstructions.* J Comp Neurol, 2005. **491**(4): p. 418-42.
19. Bernard, J.F. and J.M. Besson, *The spino(trigemino)pontoamygdaloid pathway: electrophysiological evidence for an involvement in pain processes.* J Neurophysiol, 1990. **63**(3): p. 473-90.
20. Fadok, J.P., et al., *New perspectives on central amygdala function.* Curr Opin Neurobiol, 2018. **49**: p. 141-147.
21. Petrovich, G.D. and L.W. Swanson, *Projections from the lateral part of the central amygdalar nucleus to the postulated fear conditioning circuit.* Brain Res, 1997. **763**(2): p. 247-54.

22. Penzo, M.A., V. Robert, and B. Li, *Fear conditioning potentiates synaptic transmission onto long-range projection neurons in the lateral subdivision of central amygdala.* J Neurosci, 2014. **34**(7): p. 2432-7.
23. Ciocchi, S., et al., *Encoding of conditioned fear in central amygdala inhibitory circuits.* Nature, 2010. **468**(7321): p. 277-82.
24. Li, H., et al., *Experience-dependent modification of a central amygdala fear circuit.* Nat Neurosci, 2013. **16**(3): p. 332-9.
25. Haubensak, W., et al., *Genetic dissection of an amygdala microcircuit that gates conditioned fear.* Nature, 2010. **468**(7321): p. 270-6.
26. Tye, K.M., et al., *Amygdala circuitry mediating reversible and bidirectional control of anxiety.* Nature, 2011. **471**(7338): p. 358-62.
27. Botta, P., et al., *Regulating anxiety with extrasynaptic inhibition.* Nat Neurosci, 2015. **18**(10): p. 1493-500.
28. Duvarci, S., D. Popa, and D. Pare, *Central amygdala activity during fear conditioning.* J Neurosci, 2011. **31**(1): p. 289-94.
29. Lein, E.S., et al., *Genome-wide atlas of gene expression in the adult mouse brain.* Nature, 2007. **445**(7124): p. 168-76.
30. Yu, K., et al., *Central Amygdala Somatostatin Neurons Gate Passive and Active Defensive Behaviors.* J Neurosci, 2016. **36**(24): p. 6488-96.
31. Gauriau, C. and J.F. Bernard, *Pain pathways and parabrachial circuits in the rat.* Exp Physiol, 2002. **87**(2): p. 251-8.
32. Neugebauer, V., *Amygdala pain mechanisms.* Handb Exp Pharmacol, 2015. **227**: p. 261-84.
33. Mingote, S., et al., *Functional Connectome Analysis of Dopamine Neuron Glutamatergic Connections in Forebrain Regions.* J Neurosci, 2015. **35**(49): p. 16259-71.
34. Guarraci, F.A., R.J. Frohardt, and B.S. Kapp, *Amygdaloid D1 dopamine receptor involvement in Pavlovian fear conditioning.* Brain Res, 1999. **827**(1-2): p. 28-40.
35. Guarraci, F.A., et al., *The effects of intra-amygdaloid infusions of a D2 dopamine receptor antagonist on Pavlovian fear conditioning.* Behav Neurosci, 2000. **114**(3): p. 647-51.
36. Jo, Y.S., G. Heymann, and L.S. Zweifel, *Dopamine Neurons Reflect the Uncertainty in Fear Generalization.* Neuron, 2018. **100**(4): p. 916-925 e3.
37. De Bundel, D., et al., *Dopamine D2 receptors gate generalization of conditioned threat responses through mTORC1 signaling in the extended amygdala.* Mol Psychiatry, 2016. **21**(11): p. 1545-1553.
38. Andero, R., B.G. Dias, and K.J. Ressler, *A role for Tac2, NkB, and Nk3 receptor in normal and dysregulated fear memory consolidation.* Neuron, 2014. **83**(2): p. 444-454.
39. Sanford, C.A., et al., *A Central Amygdala CRF Circuit Facilitates Learning about Weak Threats.* Neuron, 2017. **93**(1): p. 164-178.
40. Knoll, A.T., et al., *Kappa opioid receptor signaling in the basolateral amygdala regulates conditioned fear and anxiety in rats.* Biol Psychiatry, 2011. **70**(5): p. 425-33.
41. Pomrenze, M.B., et al., *Dissecting the Roles of GABA and Neuropeptides from Rat Central Amygdala CRF Neurons in Anxiety and Fear Learning.* Cell Rep, 2019. **29**(1): p. 13-21 e4.
42. Gilpin, N.W. and M. Roberto, *Neuropeptide modulation of central amygdala neuroplasticity is a key mediator of alcohol dependence.* Neurosci Biobehav Rev, 2012. **36**(2): p. 873-88.
43. Hauger, R.L., et al., *Corticotropin releasing factor (CRF) receptor signaling in the central nervous system: new molecular targets.* CNS Neurol Disord Drug Targets, 2006. **5**(4): p. 453-79.
44. DePaoli, A.M., et al., *Distribution of kappa opioid receptor mRNA in adult mouse brain: an in situ hybridization histochemistry study.* Mol Cell Neurosci, 1994. **5**(4): p. 327-35.

45. Land, B.B., et al., *The dysphoric component of stress is encoded by activation of the dynorphin kappa-opioid system.* J Neurosci, 2008. **28**(2): p. 407-14.
46. Chavkin, C., et al., *Characterization of the prodynorphin and proenkephalin neuropeptide systems in rat hippocampus.* J Neurosci, 1985. **5**(3): p. 808-16.
47. Chavkin, C., *Dynorphin--still an extraordinarily potent opioid peptide.* Mol Pharmacol, 2013. **83**(4): p. 729-36.
48. Knoll, A.T. and W.A. Carlezon, Jr., *Dynorphin, stress, and depression.* Brain Res, 2010. **1314**: p. 56-73.
49. Bruchas, M.R., et al., *CRF1-R activation of the dynorphin/kappa opioid system in the mouse basolateral amygdala mediates anxiety-like behavior.* PLoS One, 2009. **4**(12): p. e8528.
50. Sanz, E., et al., *Cell-type-specific isolation of ribosome-associated mRNA from complex tissues.* Proc Natl Acad Sci U S A, 2009. **106**(33): p. 13939-44.
51. Snyder, L.M., et al., *Kappa Opioid Receptor Distribution and Function in Primary Afferents.* Neuron, 2018. **99**(6): p. 1274-1288 e6.
52. McCullough, K.M., et al., *Quantified Coexpression Analysis of Central Amygdala Subpopulations.* eNeuro, 2018. **5**(1).
53. Bloodgood, D.W., et al., *Kappa opioid receptor and dynorphin signaling in the central amygdala regulates alcohol intake.* Mol Psychiatry, 2020.
54. Ahrens, S., et al., *A Central Extended Amygdala Circuit That Modulates Anxiety.* J Neurosci, 2018. **38**(24): p. 5567-5583.
55. Chung, S., et al., *Desipramine and citalopram attenuate pretest swim-induced increases in prodynorphin immunoreactivity in the dorsal bed nucleus of the stria terminalis and the lateral division of the central nucleus of the amygdala in the forced swimming test.* Neuropeptides, 2014. **48**(5): p. 273-80.
56. Zhu, W. and Z.Z. Pan, *Synaptic properties and postsynaptic opioid effects in rat central amygdala neurons.* Neuroscience, 2004. **127**(4): p. 871-9.
57. Chieng, B.C., M.J. Christie, and P.B. Osborne, *Characterization of neurons in the rat central nucleus of the amygdala: cellular physiology, morphology, and opioid sensitivity.* J Comp Neurol, 2006. **497**(6): p. 910-27.
58. Kang-Park, M., et al., *Interaction of CRF and kappa opioid systems on GABAergic neurotransmission in the mouse central amygdala.* J Pharmacol Exp Ther, 2015. **355**(2): p. 206-11.
59. Cole, S., R. Richardson, and G.P. McNally, *Kappa opioid receptors mediate where fear is expressed following extinction training.* Learn Mem, 2011. **18**(2): p. 88-95.
60. Xie, J.Y., et al., *Kappa opioid receptor antagonists: A possible new class of therapeutics for migraine prevention.* Cephalalgia, 2017. **37**(8): p. 780-794.
61. Nation, K.M., et al., *Lateralized kappa opioid receptor signaling from the amygdala central nucleus promotes stress-induced functional pain.* Pain, 2018. **159**(5): p. 919-928.
62. Lam, M.P. and C. Gianoulakis, *Effects of corticotropin-releasing hormone receptor antagonists on the ethanol-induced increase of dynorphin A1-8 release in the rat central amygdala.* Alcohol, 2011. **45**(7): p. 621-30.
63. Dunsmoor, J.E. and R. Paz, *Fear Generalization and Anxiety: Behavioral and Neural Mechanisms.* Biol Psychiatry, 2015. **78**(5): p. 336-43.
64. Tervo, D.G., et al., *A Designer AAV Variant Permits Efficient Retrograde Access to Projection Neurons.* Neuron, 2016. **92**(2): p. 372-382.
65. Pfeiffer, A., et al., *Anterior pituitary hormone responses to a kappa-opioid agonist in man.* J Clin Endocrinol Metab, 1986. **62**(1): p. 181-5.

66. Nabeshima, T., et al., *Stress-induced changes in brain Met-enkephalin, Leu-enkephalin and dynorphin concentrations.* Life Sci, 1992. **51**(3): p. 211-7.
67. McLaughlin, J.P., M. Marton-Popovici, and C. Chavkin, *Kappa opioid receptor antagonism and prodynorphin gene disruption block stress-induced behavioral responses.* J Neurosci, 2003. **23**(13): p. 5674-83.
68. Fadok, J.P., et al., *A competitive inhibitory circuit for selection of active and passive fear responses.* Nature, 2017. **542**(7639): p. 96-100.
69. Jo, Y.S., et al., *Persistent activation of central amygdala CRF neurons helps drive the immediate fear extinction deficit.* Nat Commun, 2020. **11**(1): p. 422.
70. Da Silva, N.L., et al., *Individual housing from rearing modifies the performance of young rats on the elevated plus-maze apparatus.* Physiol Behav, 1996. **60**(6): p. 1391-6.
71. Matthews, G.A., et al., *Dorsal Raphe Dopamine Neurons Represent the Experience of Social Isolation.* Cell, 2016. **164**(4): p. 617-31.
72. Anderson, R.I., et al., *Dynorphin-kappa opioid receptor activity in the central amygdala modulates binge-like alcohol drinking in mice.* Neuropsychopharmacology, 2019. **44**(6): p. 1084-1092.
73. Horvitz, J.C., *Mesolimbocortical and nigrostriatal dopamine responses to salient non-reward events.* Neuroscience, 2000. **96**(4): p. 651-6.
74. Pezze, M.A. and J. Feldon, *Mesolimbic dopaminergic pathways in fear conditioning.* Prog Neurobiol, 2004. **74**(5): p. 301-20.
75. Fadok, J.P., T.M. Dickerson, and R.D. Palmiter, *Dopamine is necessary for cue-dependent fear conditioning.* J Neurosci, 2009. **29**(36): p. 11089-97.
76. Jones, G.L., et al., *A genetic link between discriminative fear coding by the lateral amygdala, dopamine, and fear generalization.* Elife, 2015. **4**.
77. Heymann, G., et al., *Synergy of Distinct Dopamine Projection Populations in Behavioral Reinforcement.* Neuron, 2020. **105**(5): p. 909-920 e5.
78. Hasue, R.H. and S.J. Shammah-Lagnado, *Origin of the dopaminergic innervation of the central extended amygdala and accumbens shell: a combined retrograde tracing and immunohistochemical study in the rat.* J Comp Neurol, 2002. **454**(1): p. 15-33.
79. Groessl, F., et al., *Dorsal tegmental dopamine neurons gate associative learning of fear.* Nat Neurosci, 2018. **21**(7): p. 952-962.
80. Darvas, M., J.P. Fadok, and R.D. Palmiter, *Requirement of dopamine signaling in the amygdala and striatum for learning and maintenance of a conditioned avoidance response.* Learn Mem, 2011. **18**(3): p. 136-43.
81. Patriarchi, T., et al., *Ultrafast neuronal imaging of dopamine dynamics with designed genetically encoded sensors.* Science, 2018. **360**(6396).
82. Sun, F., et al., *A Genetically Encoded Fluorescent Sensor Enables Rapid and Specific Detection of Dopamine in Flies, Fish, and Mice.* Cell, 2018. **174**(2): p. 481-496 e19.
83. Nygard, S.K., et al., *Stress-Induced Reinstatement of Nicotine Preference Requires Dynorphin/Kappa Opioid Activity in the Basolateral Amygdala.* J Neurosci, 2016. **36**(38): p. 9937-48.
84. Schattauer, S.S., et al., *Peroxiredoxin 6 mediates Galphai protein-coupled receptor inactivation by cJun kinase.* Nat Commun, 2017. **8**(1): p. 743.
85. Stein, D.J., J.C. Ipser, and S. Seedat, *Pharmacotherapy for post traumatic stress disorder (PTSD).* Cochrane Database Syst Rev, 2006(1): p. CD002795.
86. Murrough, J.W., et al., *Emerging drugs for the treatment of anxiety.* Expert Opin Emerg Drugs, 2015. **20**(3): p. 393-406.

87. Gore, B.B., M.E. Soden, and L.S. Zweifel, *Manipulating gene expression in projection-specific neuronal populations using combinatorial viral approaches.* Curr Protoc Neurosci, 2013. **65**: p. 4 35 1-20.
88. Paxinos, G.F., K. B. J., *The Mouse Brain in Stereotaxic Coordinates*. 2008: Academic Press.